
**PROCESSING, CHARACTERIZATION AND
EROSION WEAR RESPONSE OF PARTICULATE
FILLED
ZA-27 METAL MATRIX COMPOSITES**

A THESIS SUBMITTED IN PARTIAL FULFILLMENT OF THE REQUIREMENTS
FOR THE DEGREE OF

Master of Technology
(By Research)
in
Mechanical Engineering
(Specialization: Production Engineering)

By

SRIMANT KUMAR MISHRA

Roll No.: 610ME305

Under the joint supervision of

Prof. Sandhyarani Biswas

Assistant Professor
Department of Mechanical Engineering,
National Institute of Technology,
Rourkela

Prof. Alok Satapathy

Associate Professor
Department of Mechanical Engineering
National Institute of Technology,
Rourkela



DEPARTMENT OF MECHANICAL ENGINEERING
National Institute of Technology
Rourkela, (India)

2012



National Institute of Technology Rourkela

C E R T I F I C A T E

This is to certify that the thesis entitled *Processing, Characterization and Erosion Wear Response of Particulate Filled ZA-27 Metal Matrix Composites* submitted by **SRIMANT KUMAR MISHRA** to National Institute of Technology, Rourkela for the award of the degree of **Master of Technology (By Research)** in *Mechanical Engineering* (with specialization: Production Engineering) is an authentic record of research work carried out by him under our joint guidance and supervision.

The work incorporated in this thesis has not been, to the best of our knowledge, submitted to any other University or Institute for the award of a degree or diploma.

Prof. Sandhyarani Biswas

Assistant Professor
Department of Mechanical Engineering,
National Institute of Technology,
Rourkela

Prof. Alok Satapathy

Associate Professor
Department of Mechanical Engineering,
National Institute of Technology
Rourkela

Acknowledgement

A journey is easier when you travel together. This thesis is the results of years of work whereby I have been guided and supported by many people. Hence, this would be worthwhile and pleasing to express sense of gratitude for all of them.

I would like to express my deep sense of gratitude to my supervisors ***Prof. Sandhyarani Biswas***, Assistant Professor, NIT, Rourkela and ***Prof. Alok Satapathy***, Associate Professor, NIT, Rourkela, for their invaluable guidance, motivation, untiring efforts, meticulous attention and support throughout my research work.

I am extremely thankful to **Prof. Amar Patnaik, Ms. Debasmita Mishra, Mr. Kalinga Simant Bal, Mr. Gaurav Gupta and Mr. Alok Agrawal** for their timely help during the course of this work.

My hearty thanks to madam **Mrs Susmita Satapathy** for her words of encouragement not only during the course of this work but also in my day to day walk.

It is a great pleasure for me to acknowledge and express my sincere thanks to my parents, family members and relatives for their understanding, support and encouragement that enabled me to complete this work. I am also thankful to all those who have directly or indirectly helped during my research period.

Finally, but most importantly, I am thankful to Almighty, my Lord for giving me the will power and strength to make it this far.

Date:

Place:

Srimant Kumar Mishra

TABLE OF CONTENTS

CHAPTER	CHAPTER TITLE	PAGE
	Abstract	i
	List of figures	ii
	List of tables	iv
Chapter 1	INTRODUCTION	1
1.1	Background and Motivation	1
1.2	Thesis Outline	8
Chapter 2	LITERATURE REVIEW	10
2.1	Metal Matrix Composites	10
2.2	Particulate Reinforced Metal Matrix Composite	13
2.3	Mechanical properties of the Metal matrix Composites	15
2.4	Research Reported on ZA-27 Metal Matrix Composites	18
2.5	Wear and its Classification	20
2.6	Erosion Wear Characteristics of Metal Matrix Composites	22
2.7	Implementation of Design-of-Experiments for Wear Analysis	25
2.8	Implementation of Artificial Neural Network for Wear Prediction	27
2.9	The Knowledge Gap in Earlier Investigations	29
2.10	Objectives of the Present Work	29
	Chapter Summary	30

Chapter 3	EXPERIMENTAL DETAILS	31
3.1	Materials	31
3.1.1	Matrix material	31
3.1.2	Filler materials	32
3.2	Phase Diagram of ZA-27 Alloy	35
3.3	Composite Fabrication	36
3.3.1	Techniques	36
3.3.2	Procedure	37
3.4	Mechanical Characterization	38
3.4.1	Micro-hardness measurement	38
3.4.2	X-Ray Diffraction (XRD) Studies	38
3.4.3	Tensile, flexural and impact strength measurement	38
3.5	Scanning Electron Microscopy	40
3.6	Tribological Characterization	43
3.6.1	Solid Particle Erosion Wear Test	43
3.7	Process Optimization and Taguchi Method	45
3.7.1	Taguchi Experimental Design	45
3.8	Neural Network Analysis	48
	Chapter Summary	51
Chapter 4	RESULTS AND DISCUSSION: PART-1	52
	Physical, Mechanical and Micro- Structural Characterization of the Composites	
4.1	Physical Characterization of the Composites	52
4.1.1	Density and Void Fraction	52
4.2	Mechanical Characterization of the Composites	54
4.2.1	Micro-hardness	54
4.2.2	Tensile strength	55
4.2.3	Flexural strength	56
4.2.4	Impact strength	57
4.3	X-Ray Diffraction (XRD) analysis	59
	Chapter Summary	60

Chapter 5	RESULTS AND DISCUSSION: PART-2	61
	Erosion Wear Characteristics of Al ₂ O ₃ /ZA-27 Metal Matrix Composites	
5.1	Morphology of Eroded Composite Surfaces	61
5.2	Erosion Test Results and Taguchi Analysis	62
5.3	Factor Settings for Minimum Erosion Rate	65
5.4	Analysis and Prediction of Erosion Response using ANN	67
	Chapter Summary	71
Chapter 6	RESULTS AND DISCUSSION: PART-3	72
	Erosion Wear Characteristics of SiC/ZA-27 Metal Matrix Composites	
6.1	Surfaces Morphology	72
6.2	Erosion Test Results and Taguchi Analysis	73
6.3	Factor Settings for Minimum Erosion Rate	76
6.4	Analysis and Prediction of Erosion Response using ANN	77
6.5	Comparison of Al ₂ O ₃ and SiC reinforced ZA-27 MMCs	82
	Chapter Summary	83
Chapter 7	SUMMARY AND CONCLUSIONS	84
7.1	Summary of the Research Findings	84
7.2	Conclusions	85
7.3	Recommendations for potential applications	86
7.4	Scope for future work	86
	REFERENCES	87
	APPENDICES	
	A1. Related Publications	
	A2. Brief Biodata of the Author	
	Prints of Published/Accepted Papers	

List of Figures

Figure 3.1	Different forms of available ZA-27 alloys
Figure 3.2	Commercially available alumina particles
Figure 3.3	Commercially available silicon carbide particles
Figure 3.4	Phase diagram of Zinc-Aluminium alloy
Figure 3.5	Composite fabrication steps (a-b)
Figure 3.6	Leitz Micro-hardness Tester
Figure 3.7	X'Pert X-Ray Diffractometer
Figure 3.8	Pictorial view of Universal Testing Machine Instron 1195
Figure 3.9	Loading arrangement for tensile test
Figure 3.10	Loading arrangement for three point bend test
Figure 3.11	Scanning Electron Microscope (JEOL JSM - 6480LV)
Figure 3.12	Schematic diagram of erosion test rig
Figure 3.13	Solid particle erosion trails set-up
Figure 3.14	Line diagram of artificial neural network system
Figure 4.1	Variation of composite micro-hardness with alumina content
Figure 4.2	Variation of composite micro-hardness with silicon carbide content
Figure 4.3	Variation of composite tensile strength with alumina content
Figure 4.4	Variation of composite tensile strength with silicon carbide content
Figure 4.5	Variation of composite flexural strength with alumina content
Figure 4.6	Variation of composite flexural strength with silicon carbide content
Figure 4.7	Variation of composite impact strength with alumina content
Figure 4.8	Variation of composite impact strength with silicon carbide content
Figure 4.9	X-ray diffractogram of the ZA-27 alloy
Figure 4.10	X-ray diffractogram of the Al ₂ O ₃ filled ZA-27 MMC

Figure 4.11	X-ray diffractogram of the SiC filled ZA-27 MMC
Figure 5.1	SEM micrographs of the uneroded and eroded surfaces of the ZA27 metal matrix composites filled with 9 wt% Al_2O_3
Figure 5.2	Effect of control factors on erosion rate
Figure 5.3	The three-layer neural network.
Figure 5.4	Predicted evolution of erosion rate of Al_2O_3 /ZA-27 metal matrix composites with impact velocity (at stand-off-distance 55 mm and erodent temperature 140°C)
Figure 5.5	Predicted evolution of erosion rate of Al_2O_3 /ZA-27 metal matrix composites with filler content (at stand-off-distance 55 mm and erodent temperature 140°C)
Figure 5.6	Predicted evolution of erosion rate of Al_2O_3 /ZA-27 metal matrix composites with filler content (at impact velocity 65 m/s and erodent temperature 140°C)
Figure 6.1	SEM micrographs of the uneroded and eroded surfaces of the ZA27 metal matrix composites filled with 9 wt% SiC
Figure 6.2	Effect of control factors on erosion rate
Figure 6.3	The three-layer neural network
Figure 6.4	Predicted evolution of erosion rate of SiC/ZA-27 metal matrix composites with impact velocity (at stand-off-distance 85 mm and impingement angle 45°)
Figure 6.5	Predicted evolution of erosion rate of SiC/ZA-27 metal matrix composites with filler content (at stand-off-distance 85 mm and impingement angle 45°)
Figure 6.6	Predicted evolution of erosion rate of SiC/ZA-27 metal matrix composites with stand-off-distance (at filler content 9 wt% and impingement angle 90°)
Figure 6.7	Predicted evolution of erosion rate of SiC/ZA-27 metal matrix composites with stand-off-distance (at impact velocity 35m/s and impingement angle 60°)
Figure 6.8	Comparisons between the erosion response of ZA-27/ Al_2O_3 and ZA-27/SiC MMCs under similar test conditions

List of Tables

Table 2.1	Metal matrices and reinforcements
Table 2.2	Typical thermo-mechanical properties of some metal matrices
Table 2.3	Examples of components subjected to solid particle erosion
Table 3.1	Chemical composition of ZA-27 alloy
Table 3.2	Engineering Properties of ZA-27 alloy
Table 3.3	Engineering Properties of Aluminium Oxide
Table 3.4	Engineering Properties of Silicon Carbide
Table 3.5	Parameter settings for erosion test
Table 3.6	Control factors and their selected levels (for erosion test)
Table 3.7	Taguchi orthogonal array design (L16) for solid particle erosion test
Table 4.1	Measured densities along with the porosity
Table 4.2	Mechanical properties of the composites
Table 5.1	Erosion wear test results with the corresponding S/N ratios
Table 5.2	Response table for signal to noise ratios
Table 5.3	Comparison of the experimental and the predictive erosion rates
Table 5.4	Input parameters selected for training
Table 5.5	Comparison of the experimental and the ANN predicted erosion rates of composites under similar test conditions
Table 6.1	Erosion wear test results with the corresponding S/N ratios
Table 6.2	Response table for signal to noise ratios
Table 6.3	Comparison of the experimental and the predictive erosion rates
Table 6.4	Input parameters selected for training
Table 6.5	Comparison of the experimental and the ANN predicted erosion rates of composites under similar test conditions

Chapter 1

Introduction

INTRODUCTION

1.1 Background and Motivation

Composites are combinations of two materials in which one of the materials, called the reinforcing phase, is in the form of fiber sheets or particles and are embedded in the other material called the matrix phase. The primary functions of the matrix are to transfer stresses between the reinforcing fibers/particles and to protect them from mechanical and/or environmental damage whereas the presence of fibers/particles in a composite improves its mechanical properties such as strength, stiffness etc. A composite is therefore a synergistic combination of two or more micro-constituents that differ in physical form and chemical composition and which are insoluble in each other. The objective is to take advantage of the superior properties of both materials without compromising on the weakness of either.

Composite materials have successfully substituted the traditional materials in several light weight and high strength applications. The reasons why composites are selected for such applications are mainly their high strength-to-weight ratio, high tensile strength at elevated temperatures, high creep resistance and high toughness. Typically, in a composite, the reinforcing materials are strong with low densities while the matrix is usually a ductile or tough material. If the composite is designed and fabricated correctly it combines the strength of the reinforcement with the toughness of the matrix to achieve a combination of desirable properties not available in any single conventional material. The strength of the composites depends primarily on the amount, arrangement and type of reinforcement in the resin.

Broadly, composite materials can be classified into three groups on the basis of matrix material. They are:

- (a) Polymer Matrix Composites (PMC)
- (b) Ceramic Matrix Composites (CMC)
- (c) Metal Matrix Composites (MMC)

a) Polymer Matrix Composites:

Most commonly used matrix materials are polymeric. The reasons for this are two-fold. In general the mechanical properties of polymers are inadequate for many structural purposes. In particular their strength and stiffness are lower compared to metals and ceramics. These difficulties are overcome by reinforcing other materials with polymers. Secondly the processing of polymer matrix composites need not involve high pressure and does not require high temperature. Also, equipments required for manufacturing polymer matrix composites are simpler. For this reason polymer composites developed rapidly and soon became popular for structural applications. Polymer composites are used because overall properties of the composites are superior to those of the individual polymers. They have a greater elastic modulus than the neat polymer but are not as brittle as ceramics.

b) Ceramic Matrix Composites:

One of the main objectives in producing ceramic matrix composites is to increase the toughness. Naturally it is hoped and indeed often found that there is a concomitant improvement in strength and stiffness of ceramic matrix composites.

c) Metal Matrix Composites:

Metal matrix composites have many advantages over monolithic metals like higher specific modulus, higher specific strength, better properties at elevated temperatures and lower coefficient of thermal expansion. Because of these attributes metal matrix composites are under consideration for wide range of applications viz. combustion chamber nozzle (in rocket, space shuttle), housings, tubing, cables, heat exchangers, structural members etc.

Thus, a *metal matrix composite* (MMC) is composite material with at least two constituent parts, one being a metal. The other material may be a different metal or another material, such as a ceramic or organic compound. When at least three materials are present, it is called a hybrid composite. An MMC is complementary to a cermet. MMCs are made by dispersing a reinforcing material into a metal matrix. The reinforcement surface can be coated to prevent a chemical reaction with the matrix. For example, carbon fibers are commonly used in aluminum matrix to synthesize composites showing low density and high strength. However, carbon reacts with aluminum to generate a brittle and water-soluble compound Al_4C_3 on the surface of the fiber. To prevent this reaction, the carbon fibers are coated with nickel or titanium boride.

The matrix is the monolithic material into which the reinforcement is embedded, and is completely continuous. This means that there is a path through the matrix to any point in the material, unlike two materials sandwiched together. In structural applications, the matrix is usually a lighter metal such as aluminum, magnesium, or titanium, and provides a compliant support for the reinforcement. In high temperature applications, cobalt and cobalt-nickel alloy matrices are common.

The reinforcement material is embedded into the matrix. The reinforcement does not always serve a purely structural task (reinforcing the compound), but is also used to change physical properties such as wear resistance, friction coefficient, or thermal conductivity. The reinforcement can be either continuous or discontinuous. Discontinuous MMCs can be isotropic, and can be worked with standard metalworking techniques, such as extrusion, forging or rolling. In addition, they may be machined using conventional techniques, but commonly would need the use of polycrystalline diamond tooling (PCD).

Continuous reinforcement uses mono-filament wires or fibers such as carbon fiber or silicon carbide. Because the fibers are embedded into the matrix in a certain direction, the result is an anisotropic structure in which the alignment of

the material affects its strength. One of the first MMCs used boron filament as reinforcement. Discontinuous reinforcement uses "whiskers", short fibers, or particles. The most common reinforcing materials in this category are alumina and silicon carbide [1].

Carbide drills are often made from a tough cobalt matrix with hard tungsten carbide particles inside. Some tank armors may be made from metal matrix composites, probably steel reinforced with boron nitride. Boron nitride is a good reinforcement for steel because it is very stiff and it does not dissolve in molten steel. Some automotive disc brakes use MMCs. Early Lotus Elise models used aluminum MMC rotors, but they have less than optimal heat properties and Lotus has since switched back to cast-iron. Modern high-performance sport cars, such as those built by Porsche, use rotors made of carbon fiber within a silicon carbide matrix because of its high specific heat and thermal conductivity. *Ford* offers a metal matrix composite driveshaft upgrade. The MMC driveshaft is made of an aluminum matrix reinforced with boron carbide, allowing the critical speed of the driveshaft to be raised by reducing inertia. The MMC driveshaft has become a common modification for racers, allowing the top speed to be increased far beyond the safe operating speeds of a standard aluminum driveshaft. *Honda* has used aluminum matrix composite cylinder liners in some of their engines, including the B21A1, H22A and H23A, F20C and F22C, and the C32B used in the NSX. *Toyota* has since used metal matrix composites in the *Yamaha*-designed 2ZZ-GE engine which is used in the later Lotus Elise S2 versions as well as Toyota car models, including the eponymous Toyota Matrix. *Porsche* also uses MMCs to reinforce the engine's cylinder sleeves in the *Boxster* and *911*. The *F-16 Fighting Falcon* uses mono-filament silicon carbide fibers in a titanium matrix for a structural component of the jet's landing gear.

MMCs are nearly always more expensive than the more conventional materials they are replacing. As a result, they are found where improved properties and performance can justify the added cost. Today these applications are found most

often in aircraft components, space systems and high-end or "boutique" sports equipment. The scope of applications will certainly increase as manufacturing costs are reduced.

In comparison with conventional polymer matrix composites, MMCs are resistant to fire, can operate in wider range of temperatures, do not absorb moisture, have better electrical and thermal conductivity, are resistant to radiation damage, and do not display out-gassing. On the other hand, MMCs tend to be more expensive, the fiber-reinforced materials may be difficult to fabricate, and the available experience in use is limited. However, the advantages of these composite materials are only realized when there is a reasonable cost – performance relationship in the component production.

Reinforcements for metal matrix composites have a manifold demand profile, which is determined by production and processing and by the matrix system of the composite material. The following demands are generally applicable: low density, mechanical compatibility (a thermal expansion coefficient which is low but adapted to the matrix), chemical compatibility, thermal stability, high Young's modulus, high compression and tensile strength, good processability and economic efficiency. These demands can be achieved only by using non-metal/inorganic reinforcement components. For metals, ceramic particles or, rather, fibers or carbon fibers are often used. Due to the high density and the affinity to reaction with the matrix alloy, the use of metallic fiber usually fails. Which components are finally used, depends on the selected matrix and on the demand profile of the intended application. The production, processing and type of application of various reinforcements depend on the production technique for the composite materials. A combined application of various reinforcements is also possible (hybrid technique) [2].

The selection of suitable matrix material is mainly determined by the intended application of the composite material. With the development of light metal composite materials that are mostly easy to process, conventional light metal

alloys are applied as matrix materials. In the area of powder metallurgy, special alloys can be applied due to the advantage of fast solidification during the powder production. Those systems are free from segregation problems that arise in conventional solidification.

Metal matrix composites are often used as engineering as well as structural components functioning in hostile workplaces where they are subjected to different wear situations. *Wear* is defined as the damage to a solid surface usually involving progressive loss of materials, owing to relative motion between the surface and a contacting substance or substances [3]. It is a material response to the external stimulus and can be mechanical or chemical in nature. The effect of wear on the reliability of industrial components is recognised widely and the cost of wear has also been recognised to be very high. Systematic efforts in wear research were started in 1960s in industrialized countries. The direct costs of wear failures (i.e. wear part replacements), increased work and time, loss of productivity as well as indirect losses of energy and the increased environmental burden are real problems in everyday work and business. In catastrophic failures, there is also the possibility of human losses. Although wear has been extensively studied scientifically, still wear problems persist in industrial applications. This actually reveals the complexity of the wear phenomenon [4].

There are quite a few terms to describe various wear modes which can be clubbed into four principal categories viz. abrasion, adhesion, erosion and surface fatigue [5]. Generally, abrasive wear occurs when two surfaces in contact move against each other and the harder particle in one cut through the other. This form of wear comes into play when a tangential motion causes the material removal by the simultaneous micro-ploughing and micro-cutting [3]. However, wear due to localised bonding between contacting solid surfaces leading to material transfer between the two surfaces or the loss from either surface is termed as adhesive wear. Similarly, surface fatigue is another wear

process that takes place when tiny wear particles are dislodged from a surface by fracture on repeated rolling or sliding on the surface. Owing to a repeated loading action subsurface cracks grow from pre-existing defects, join hands with other vicinal cracks and finally come to the surface removing a small chunk of material [5]. Finally in the erosion wear mode, a progressive loss of material occurs from a solid surface due to mechanical interaction between that surface and a fluid, a multi-component fluid, or impinging liquid or solid particles [6].

Solid particle erosion (SPE), a typical erosion wear mode, is the loss of material that results from repeated impact of small, solid particles. In some cases SPE is a useful phenomenon, as in sandblasting and high-speed abrasive water jet cutting but it is a serious problem in many engineering systems including steam and jet turbines, pipelines and valves carrying particulate matter and fluidized bed combustion systems. Solid particle erosion is to be expected whenever hard particles are entrained in a gas or liquid medium impinging on a solid at any significant velocity. In both cases, particles can be accelerated or decelerated and their directions of motion can be changed by the fluid.

Metals and metal based composites form a very important class of tribo-engineering materials and are invariably used in mechanical components, where wear performance in non-lubricated condition is a key parameter for the material selection. Nowadays much attention is devoted towards the study of solid particle erosion behaviour of such composites due to the high potential use of these materials in many mechanical and structural applications. Hence, erosion resistance of composites has become an important material property, particularly in selection of alternative materials and therefore the study of solid particle erosion characteristics of these composites has become highly relevant. Differences in the erosion behaviour of various types of composite materials are caused by the amount, type, orientation and properties of the reinforcement on one hand and by the type and properties of the matrix and its adhesion to the fibers/fillers on the other hand. A full understanding of the effects of all system

variables on the wear rate is necessary in order to undertake appropriate steps in the design of machine or structural component and in the choice of materials to reduce/control wear [7].

Statistical methods have commonly been used for analysis, prediction and/or optimization of a number of engineering processes. Such methods enable the user to define and study the effect of every single condition possible in an experiment where numerous factors are involved. Solid particle erosion is a complex wear phenomenon in which a number of control factors collectively determine the performance output (i.e. the erosion rate) and there is enormous scope in it for implementation of appropriate statistical techniques for process optimization. But unfortunately, such studies have not been adequately reported so far. The present research work addresses to this aspect by adopting a statistical approach called Taguchi experimental design. Like any experimental investigation, erosion trials on composites also demand substantial amount of time, energy and materials. Hence, there is a need for a prediction tool to supplement to the experiments. In the present study, a model based on artificial neural network (ANN) is implemented to predict erosion rate of the composites subjected to different operating conditions.

Against this background, the present research work is undertaken to study the effects of particulate fillers on the solid particle erosion response of ZA-27 alloy based metal matrix composites.

1.2 Thesis Outline

The remainder of this thesis is organized as follows:

Chapter 2: Includes a literature review designed to provide a summary of the base of knowledge already available involving the issues of interest. It presents the research works on wear behavior of metal matrix composites by various investigators.

- Chapter 3:** Includes a description of the raw materials and the test procedures. It presents the details of fabrication and characterization of the composites under investigation and also an explanation of the Taguchi experimental design and neural computation.
- Chapter 4:** Presents the physical and mechanical properties of the composites under study.
- Chapter 5:** Presents the experimental findings on the erosion characteristics of $\text{Al}_2\text{O}_3/\text{ZA 27}$ composites.
- Chapter 6:** Presents the experimental findings on the erosion characteristics of $\text{SiC}/\text{ZA 27}$ composites.
- Chapter 7:** Provides summary of the findings of this research work, outlines specific conclusions drawn from the experimental efforts and suggests ideas and directions for future research.

Chapter 2

Literature Review

LITERATURE REVIEW

In the current chapter, the summary of the literature surveyed during the course of this research has been presented. This survey of literature is expected to provide the background information and thus to select the objectives of the present investigation. A treatise on metal matrix composites (MMCs) and particulate filled MMCs has been given illustrating the previous research findings. A brief research history on ZA-27 metal matrix composites is also provided. In short, this treatise embraces various aspects of metal matrix composites with a special reference to their physical, mechanical and tribological characteristics. This chapter thus includes reviews of available research reports:

- ❖ On Metal Matrix Composites
- ❖ On Particulate Reinforced Metal Matrix Composites
- ❖ On Mechanical Properties of MMCs
- ❖ On Research Reported on ZA-27 Metal Matrix Composites
- ❖ On Wear and its Classification
- ❖ On Erosion Wear of MMCs
- ❖ On Implementation of Design-of-Experiments for Wear Analysis
- ❖ On Implementation of Artificial Neural Network for Wear Prediction

2.1 Metal Matrix Composites

Polymer composites are used normally up to 180⁰C, but rarely beyond 350⁰C. The high temperature capabilities of inorganic reinforcements cannot be realized, when polymers are employed as matrix materials. Metal matrices, on the other hand, can widen the scope of using composites over a wide range of temperatures. Besides, metal matrix composites allow tailoring of several useful properties that are not achievable in conventional metallic alloys. High specific strength and stiffness, low thermal expansion, good thermal stability and improved wear resistance are some of the positive features of metal matrix

composites. The metal composites also provide better transverse properties and higher toughness compared to polymer composites. Table 2.1 provides the list of some metal matrices and associated reinforcing materials. The reinforcements can be in the form of either particulates, or short fibers or continuous fibers. Cermets constitute an important group of metal matrix composites in which ceramic grains of sizes greater than 1 μm are dispersed in the refractory metal matrix. A typical example is the titanium carbide cermet which comprises of 70% TiC particles and 30% nickel matrix and exhibits high specific strength and stiffness at very high temperatures. The thermo-mechanical properties of some common matrices are presented in Table 2.2. The aluminium matrices include several alloys such as AA1100, AA2014, AA6061, AA7075, AA5052 etc. The composites with aluminium matrices are relatively lightweight, but their applications are limited to the lower temperature range because of its low melting point. There are several systems such as engine components which are exposed to high level of temperature. Titanium and nickel composites are ideal for such situations, as they retain useful properties at 1000-1100⁰C. Super alloys, NiCrAlY and FeCrAlY, are also used as matrices because of their high oxidation resistance properties. Molybdenum is a high temperature matrix and fiber material. Iron and steel matrices are cheaper and can be used at high temperatures, if the weight is not the major concern.

Table 2.1: Metal matrices and reinforcements

Matrix	Reinforcements
Aluminium and alloys	C, Be, SiO ₂ , B, SiC, Al ₂ O ₃ , Steel, B ₄ C, Al ₃ Ni, Mo, W, ZrO ₂
Titanium and alloys	B, SiC, Mo, SiO ₂ , B _e , ZrO ₂
Nickel and alloys	C, B _e , Al ₂ O ₃ , SiC, Si ₃ N ₄ , steel, W, Mo, B
Magnesium alloys	C, B, glass, Al ₂ O ₃
Molebdenum and alloys	B, ZrO ₂
Iron and Steel	Fe, Steel, B, Al ₂ O ₃ , W, SiO ₂ , ZrO ₂
Copper and alloys	C, B, Al ₂ O ₃ , E-glass

Table 2.2: Typical thermo-mechanical properties of some metal matrices

Matrices	Density kg/m ³	Tensile strength MPa	Tensile modulus GPa	Coefficient thermal expansion 10 ⁻⁶ m/mk	Thermal conductivity W/(mk)	Heat capacity KJ/ (kg.k)	Melting point °C
AA6061	2800	310	70	23.4	171	0.96	590
Nickel	8900	760	210	13.3	62	0.46	1440
Ti-6AL-4V	4400	1170	110	9.5	7	0.59	1650
Magnesium	1700	280	40	26	100	1.00	570
Steel	7800	2070	206	13.3	29	0.46	1460
Copper	8900	340	120	17.6	391	0.38	1080

Metal matrix composites (MMCs) have recently become candidates for critical structural applications because of a combination of superior mechanical properties such as better elastic modulus, tensile strength, high temperature stability and wear resistance in comparison with the parent matrix alloys. Discontinuous MMCs, i.e. materials containing a discontinuous reinforcement such as short fibers, whiskers or particles, have been reported to have the greatest potential [8]. MMCs offer designers benefits as they are particularly suited for applications requiring good strength at high temperature, good structural rigidity, dimensional stability and light weight. The present day trend is towards safe usage of the MMC parts in the automobile engines, which work particularly at high temperature and pressure environments [9]. The increase in demand for lightweight, stiff and strong materials has led to the development of MMCs reinforced with ceramic dispersoids. These MMCs possess excellent mechanical and tribological properties and are considered as potential engineering materials for various tribological applications. Several researchers have worked on sliding wear mechanism of MMCs reinforced with ceramic particulates like SiC, Al₂O₃ and garnet particles etc. and have observed improvement in wear and abrasion resistance [10]. Rohatgi [11] reviewed the

world-wide upsurge in metal-matrix composite research and development activities with particular emphasis on cast metal-matrix particulate composites. Bandyopadhyay et al. [12] highlighted the development and processing of new generation metal matrix composites. Chou et al. [13] reported a review on fiber reinforced metal matrix composites. They studied the fabrication methods, mechanical properties, secondary working techniques and interfaces of those MMCs. Some researchers reported on the finite element modeling of metal matrix composites [14-16]. Many research works, in recent years, have actually been carried out on different properties and wear response of particulates reinforced metal matrix composites [17-21].

2.2 Particulate Reinforced Metal Matrix Composite

Particulate reinforced metal matrix composites have been used extensively in various fields due to their cost-effectiveness, high interfacial bonding and easy to form into complex shapes. Besides, they behave isotropically and are not as sensitive as long fiber composites to the mismatch of thermal expansion between the matrix and the reinforcement [22, 23]. Generally particulate fillers are used in metal matrix for a variety of reasons such as cost reduction, improved processing, density control, thermal conductivity, control of thermal expansion, electrical properties, magnetic properties, improved hardness and better wear resistance.

Hard particulate fillers consisting of ceramic or metal particles such as SiC, Al₂O₃, graphite, aluminium diboride, cemented carbide, tungsten carbide, niobium carbide, NiAl, TiC, Si₃N₄, MoSi₂, Mg, TiB₂ etc. are being used these days to improve the performance of metal matrix composites to a great extent [24-30]. Some researchers try to utilize the industrial waste like fly ash [31, 32], red mud [33] and copper slag as a reinforcement to improve certain properties of the metal matrix composites. The mechanical properties of particulate/metal matrix composites depend strongly on the particle size, particle-matrix interface adhesion and particle loading. Efforts have been made towards improving the

elevated temperature properties of the alloy system through alloying with high melting elements like Mn, Ni, and Si or by means of dispersing hard second phase particles [34]. Hard and thermally stable ceramic reinforcement in ZA alloys contributes to a higher hardness, superior elastic modulus and lower coefficient of thermal expansion of the matrix alloy at ambient temperature [35]. In the case of particulate reinforcement, Cornie et al. and Karni et al. indicated that the presence of SiC particles in ZA alloys leads to a substantial improvement in elastic modulus and hardness [36]. Tjong [37] studied the influence of Al-based and Mg-based nano-particle to enhance mechanical properties. Doe et al. [38] reported that 0.2% proof stress, tensile strength and ductility fall as particle size increases. Pardo et al. [39] studied Influence of reinforcement grade on corrosion resistance of cast aluminum matrix composites. Jayamathy et al. [17] investigated the influence of SiC reinforcement on wear response of Mg alloys. The effect of volume fraction of reinforcement and their interfacial bonding on erosion rate of copper/SiC metal matrix composite has been studied by Chen et al. [40].

Usually, the strength of a composite strongly depends on the stress transfer between the particles and the matrix [41]. For well-bonded particles, the applied stress can be effectively transferred to the particles from the matrix resulting in an improvement in the strength. However, for poorly bonded micro-particles, reduction in strength is found to have occurred. Ilegbusi et al. [42] investigated porosity nucleation in metal matrix composite and reported that reinforcement coatings such as Cu coating on SiC significantly reduces the contact angle, enhance wettability at the interface. Shoukry et al. [16] studied the microscopic and macroscopic response of a particulate reinforced MMC using finite element analysis. Various kinds of such metal matrix composites reinforced with metal particles are finding a wide range of applications such as components in automotive, aerospace, opto-mechanical assemblies, thermal management, fan exit guide vane (FEGV) in the gas turbine engine, ventral fins and fuel access cover doors in military aircraft and rotating blade sleeves in helicopters etc. [43].

2.3 Mechanical properties of the Metal matrix composites

Properties of composite material can be considered under two headings (a) those that depend solely upon the geometrical arrangement of the phases and their respective volume fractions and not at all upon the dimensions of the components and those depend on structural arrangements such as periodicity of arrangements or the sizes of the pieces of the two or more component phases. Indeed, in many instances the properties of phases making the composite start changing when the smallest dimension of the phase falls below a certain dimension. From the literature review, it is seen that the mechanical properties of metal matrix composites are dependent on the type and volume fraction of the reinforcement, dislocation strengthening and the defects introduced during the fabrication of MMCs. Most widely considered property in MMCs are its tensile strength, ductility, hardness and fracture. The investigations of various researchers in this area are as follows:

Chawla et al. [44] have reported that the incorporation of particle in the matrix and increase in volume fraction of the reinforcement improve the tensile strength, and elastic modulus but at the cost of ductility. With increase in volume fraction more load gets transferred to reinforcement which leads to increase in ultimate tensile strength, the work hardening rate increases with increase in volume fraction and lower ductility can be attributed to void nucleation with increased amount reinforcement and cracked particle in the composite because of processing of composite. Sharma et al. [45] reported that the properties of discontinuously reinforced composites are strongly dependent on many variables including the distribution of the particles in the matrix, the mechanical properties of the matrix and the reinforcing particles and the interfacial bond between the matrix and reinforcement. As per the observation reported by Van Stone [46], in aluminium matrix composites, Young's modulus increases with increase in the content of reinforcing material regardless of the type of reinforcement used. Poddar [47] made a study on AZ91D alloy (magnesium alloy) reinforced with SiC particulates and reported that the

presence of particulate increases the yield strength and Young's modulus of the parent material. The basic mechanism of composite deformation is the load transfer from matrix to reinforcement and a good bonding between matrix and reinforcement gives rise to better load transfer and improved properties. Sharma et al. [48] have further reported that the presence of hard Zirconium particulate imparts strength to ZA-27 matrix leading to more resistance against the applied tensile load. In the case of particle-reinforced composites, there is a restriction to the plastic flow as a result of dispersion of the hard particles in the matrix, thereby providing enhanced tensile strength in the composite.

Sharma et.al [49] found that the addition of quartz particles had positive effect on lead alloy as it increases the hardness, ultimate tensile strength, impact strength but at the cost of ductility. Increase in hardness is due to the fact that quartz particle is a hard dispersoid and these particles act as barriers for the movement of dislocations and hence increase the hardness. The increase in ultimate tensile strength is due to the presence of hard particle which impart strength to soft matrix. The increase in quartz content reduces the inter particle distance between these hard particles causing increase in the dislocation pile up and there is a restriction to the plastic flow due to the dispersion of these particles. Kok [50] reported that the mechanical properties such as tensile strength, hardness increase and elongation decreases with decreasing size of the particle and increasing the volume fraction and also the density of the composites increased with increasing weight percentage and size of the particle where as the porosity of the composites increased with decreasing size and increasing weight percentage of particles. Abdizadeh et al. [51] found that with increase in zircon content and increase in sintering temperature the hardness of the metal matrix composite increases. With random distribution of zircon particles they agglomerate in a region and would not change during sintering with increase in zircon content and the direct contact between these regions causes weak binding between the boundaries and thus reduces the strength of the composites.

Kaataih et al. [52] found that the addition of TiO_2 particles has significant effect on mechanical properties of the MMCs because with increase in reinforcement content the ultimate tensile strength, yield strength and hardness of the composite increase while the ductility of the composite decreases. Increase in hardness is due to the hard TiO_2 particles acting as barriers to the movement of dislocation and contribute positively to the hardness of the composites and decrease in ductility can be attributed to the embrittlement effect of hard TiO_2 particle which causes increased local stress concentration sites. So there is a necessity of a compromise with the amount of reinforcement in the composite to enhance the mechanical properties. Mares [53] found that, it is possible to optimize the properties of metal matrix composites for which he considered Al matrix reinforced by graphite and SiC particle and studied the mechanical properties under different heat treatment conditions. He concluded that heat treatment has the potential to produce desired mechanical properties in aluminium-graphite composites. And by choosing optimum volume fraction of reinforcement and the heat treatment duration, the mechanical properties of the metal matrix composites can be optimized. Most of the studies reported on metal matrix composites reveal that their mechanical properties are strongly influenced by many factors such as weight fraction of the reinforced particles, their distribution in the matrix and also their properties. Few studies reported that the mechanical properties of the metal matrix composites are dependent on volume fraction of the fibers, fiber aspect ratio, fiber-matrix adhesion etc. The effect of heat treatment on mechanical properties is also reported by some researchers [54, 55].

Several investigations have been made on mechanical properties of metal matrix composites reinforced with a wide range of particulate materials such as tungsten carbide, copper, fly ash, silicon carbide, silicon, alumina, graphite, manganese etc. Prasad et al. [56] reported on improvement in hardness of modified zinc-base alloy by reinforcing Ni and Si, whereas report shows decrease in density. Cuvalc et al. [57] studied the mechanical properties of

ZnAl27Cu2Si2 alloy containing 2% Si and reported maximum tensile strength of 325 Mpa and hardness of 125 HB. Badish et al. [58] evaluated the mechanical behavior of tungsten carbide reinforced metal matrix composites. Seenappa et al. [59] found that hardness, tensile strength, yield strength and density increases with increase in copper content but impact strength decreases after 2 wt% of copper. Modi et al. [60] developed composite using alumina particles and reported that hardness value shows improvement than the base alloy whereas the density, tensile strength and elongation followed a reverse trend. Dominguez et al. [61] studied the influence of manganese on the strength of ZA-27 alloy. Chen et al. [62] presented that the hardness of the composites continuously decreased with the increase of silicon content. The main reason behind this should be the increase in porosity with the increase in silicon content [63]. Bobic et al. [64] reported on effect of alumina reinforcement on strength of ZA-27 based composite. Mechanical properties such as yield strength and hardness of ZA-27 alloy increase significantly but at the cost of ductility by reinforcing titanium dioxide as reported by Ranganath et al. [65] and by adding zircon particles as reported by Sharma et al. [66].

2.4 Research Reported on ZA-27 Metal Matrix Composites

ZA-27 is the lightest alloy and offers excellent bearing and wear resistance properties. It is also the high strength performer of the zinc alloys originally developed as a high strength gravity casting alloy and was suitable for thin wall die casting [65]. Its friction and wear characteristics can compare to the standard bearing material of industrial SAE660 lead-tin bronze [65]. Apart from its use as thin wall castings and in components such as electrical, automotive, industrial and farm equipment, it is increasingly popular in the markets for bearings, wear-resisting parts, valves, pulleys and sheaves [55]. Due to good tribo-mechanical properties, low weight, excellent foundry castability and fluidity, good machining properties, high as-cast strength and hardness, corrosion resistance, low initial cost, energy-saving melting, environmental friendly technology, and equivalent or even superior bearing and wear properties, the ZA alloys (mostly

ZA-12 and ZA-27) are capable of replacing aluminum cast alloys and bearing bronzes [67]. An important aspect that makes these alloys attractive is the reductions in cost from 25 to 50% and 40 to 75%, compared with aluminum and brass alloys respectively [9]. However, major limitations of the alloy system are its inferior elevated temperature mechanical and wear properties, dimensional instability at temperature above 100⁰ C [36,62]. Efforts have been made towards improving the elevated temperature properties of the alloy system through alloying with high melting elements like Mn, Ni, and Si or by means of dispersing hard second phase particles [34]. Hard and thermally stable ceramic reinforcement in ZA alloys contributes to a higher hardness, superior elastic modulus and lower coefficient of thermal expansion of the matrix alloy at ambient temperature [35].

Several researchers reported on the mechanical and tribological behavior of ZA-27 metal matrix composites reinforced with particulates or short fibers fillers. Sharma et al. [68], in 1996, reported on the effect of short glass fibers on mechanical properties of ZA-27 alloy composites. Again in 1998, they studied the aging characteristics of the same composites [69]. In 2001, Sharma [70] studied the elastic properties of ZA-27 alloy composites reinforced with short glass fibers using destructive test. He also made some prediction of analytical value using shear-lag model, Nielsen-Chen model, and computational model. Some reports on the wear behavior of ZA-27 metal matrix composites reinforced with different particulate filler like SiC [71], alumina [72], garnet [9], Mn [55], silicon [62], zircon [66] and graphite [73] etc. Ranganath et al. [65] and Sharma et al. [66] studied the mechanical properties and fractography of ZA-27 MMCs reinforced with titanium dioxide and zircon particle respectively. Seah et al. [74] in 1996, investigated the mechanical properties of cast ZA-27/graphite particulate composites. Again in 1997, they compared the mechanical properties of as cast and heat-treated ZA-27/graphite particulate composites [54]. Very recently, Patnaik et al. [75] investigated the solid particle erosion of ZA-27 alloy matrix composites reinforced with titania particles.

2.5 Wear and its Classification

Wear is the process occurring at the interfaces between interacting bodies and is usually hidden from investigators by the wearing components. However, this obstacle has been gradually overcome by scientists, revealing an intricate world of various wear modes and mechanisms. The widest definition of wear, which has been recognized for at least 50 years, includes the loss of material from a surface, transfer of material from one surface to another or movement of material within a single surface [76]. Although a narrower definition of wear has been proposed as progressive loss of substances from the operating surface of a body occurring as a result of relative motion at the surface [77], the wide range of engineering applications of concern to the tribologists is served better by a broader definition. A simple and useful statement is that wear is damage to a solid surface, generally involving progressive loss of material, due to relative motion between that surface and a contacting substance or substances [3]. This includes:

1. Degradation by the displacement of material within the surface (leading to changes in surface topography without loss of material), as well as the more usual case of material removal,
2. The wear processes common in machines in which one surface slides or rolls against another, either with or without the presence of a deliberately applied lubricant, and
3. The more specialized types of wear which occur when the surface is abraded by hard particles moving across it, or is eroded by solid particles or liquid drops striking it or by the collapse of cavitation bubbles in a liquid.

This definition, quite deliberately tells nothing about the mechanisms by which the degradation takes place. These may be purely mechanical, for example involving plastic deformation or brittle fracture or they may involve significant chemical aspects, like oxidation of a metal or hydration of a ceramic; in many practical cases, both chemical and mechanical processes play a role [78].

A fundamental scheme to classify wear was first outlined by Burwell and Strang [79]. Later, Burwell [80] modified the classification to include five distinct types of wear, namely:

1. Abrasive wear: Abrasive wear or abrasion is generally defined as the wear that is caused by the displacement of material from a solid surface due to hard particles sliding along the surface and cutting grooves on the softer surfaces. It accounts for most failures in practice. This hard material may originate from one of the two surfaces, rubbing against each other. In sliding mechanisms, abrasion can arise from the existing asperities on one surface (if it is harder than the other), from the generation of wear fragments which are repeatedly deformed and hence get work hardened or oxidized until they become harder than either or both of the sliding surfaces or from the adventitious entry of hard particles, such as dirt from outside the system.

2. Adhesive wear: Adhesive wear can be defined as wear due to localized bonding between contacting solid surfaces leading to material transfer between the two surfaces or the loss from either surface. For adhesive wear to occur it is necessary for the surfaces to be in intimate contact with each other. Surfaces, which are held apart by lubricating films, oxide films etc. reduce the tendency for adhesion to occur.

3. Surface fatigue: Wear of a solid surface can also be caused by fracture arising from material fatigue. The term fatigue is broadly applied to the failure phenomenon where a solid is subjected to cyclic loading involving tension and compression above a certain critical stress. Repeated loading causes the generation of micro-cracks, usually below the surface, at the site of a pre-existing point of weakness. On subsequent loading and unloading, the micro-crack propagates. Once the crack reaches the critical size, it changes its direction to emerge at the surface and thus flat sheet like particles is detached during wearing. The number of stress cycles required to cause such failure decreases as the corresponding magnitude of stress increases. Vibration is a common cause of fatigue wear.

4. Corrosive wear: Most metals are thermodynamically unstable in air and react with oxygen to form an oxide, which usually develop layer or scales on the surface of metal or alloys when their interfacial bonds are poor. Corrosion wear is the gradual eating away or deterioration of unprotected metal surfaces by the effects of the atmosphere, acids, gases, alkalis etc. This type of wear creates pits and perforations and may eventually dissolve metal parts.

5. Erosive wear: In tribology, erosive wear can be defined as the progressive loss of original material from a solid surface due to mechanical interaction between the surface and impinging particles. Erosive wear is caused by the impact of particles of solid or liquid against the surface of an object. It occurs in a wide variety of machinery and typical examples are the damage to gas turbine blades when an aircraft flies through dust clouds and the wear of pump impellers in mineral slurry processing systems. In common with other forms of wear, mechanical strength does not guarantee wear resistance and a detailed study of material characteristics is required for wear minimization. The properties of the eroding particle are also significant and are increasingly being recognized as a relevant parameter in the control of this type of wear. Erosive wear involves several wear mechanisms which are largely controlled by the particle material, the angle of impingement, the impact velocity and the particle size. If the particle is hard and solid then it is possible that a process similar to abrasive wear will occur. Where liquid particles are the erodent, abrasion does not take place and the wear mechanisms involved are the result of repetitive stresses on impact. The term 'erosive wear' refers to an unspecified number of wear mechanisms which occur when relatively small particles impact against mechanical components. This definition is empirical by nature and relates more to practical considerations than to any fundamental understanding of wear.

2.6 Erosion Wear Characteristics of Metal Matrix Composites

Erosion wear by solid particle/erodent are one of the most prominent problem in industries like refineries, metallurgical units, steam turbines etc. Consequently, a huge loss of economic value associated with such kind of wear is smashing the financial budgets of the industries in particular and the country as a whole. Thus,

it becomes a challenge for engineers and material scientists to develop either such a material that adaptively arrests erosion to the best extent possible or to develop such theoretical/ simulated models that provides quality judgement to anticipate the rate of erosion so that precautions could be taken in preliminary stages of research/development itself. Research in the 1950s and 1960s produced significant new concepts and formed the building blocks of understanding in the areas of sliding, fretting, abrasive, and erosive wear. Concepts of adhesion, the true area of contact, interfacial transfer, critical angles for maximum abrasion and erosion, and the mechanics of contact of rough surfaces were all advanced during that period as well.

Aquaro [81], classified the variables affecting the erosion wear into three types:

1. Impingement variables describing the particle flow:

- Particle velocity
- Angle of impact
- Particle concentration

2. Particle variables:

- Particle shape
- Particle density
- Particle size

3. Material variables

- Young's modulus
- Poisson's ratio
- Plastic behaviour
- Failure behavior

Lindesly [82], in his work on solid particle erosion of an Fe-Fe₃C metal matrix composite, in which Fe-C system was considered as alloy matrix and martensite (Fe₃C) as reinforcement concluded that the erosion resistance increases as there is decrease in inter-particle spacing. He also showed the dependence of both particle size and volume fraction on erosion rate. As the particle size decreases, the erosion rate decreases and increase in volume fraction of reinforcement also

decreases the erosion rate. Das et.al [83] found that as cast Al alloy shows higher erosion rate in comparison with heat treated Al alloy irrespective of impingement angle. The material loss during erosive wear is due to micro-cutting/micro-plowing and micro-fracture. At low impingement angle, the material loss is due to micro-cutting/micro-plowing and at higher impingement angle, it is due to both micro-fracture and micro-cutting/micro-plowing. Fang et al.[84] reported that the erosion resistance depends on the bonding strength between matrix and particle and the erosion resistance of Al MMC reinforced with particle or fiber can be enhanced by use of high specific strength Al alloy and erosion resistant fibers. Similarly, Zhou et al. [85] has also reported similar observations.

Modi et al. [34] showed that the erosion wear resistance of composites is higher than that of the matrix alloys as the composites exhibit less subsurface damage than the matrix alloys. Flores et al. [86] conducted an experimental study and reported extensively on erosion-corrosion wear behaviour of MMCs. Kondoh et al. [87] found that AlN particles were effective in improving the erosion resistance of composites as there is a good interfacial bond between matrix and the particles. Das et al. [88] noted that the higher wear rate at normal impingement angle on the surface may be due to higher degree of nominal impact energy offered by the erodent on the specimen surface and found that interface between alloy and hard particle plays an important role. Chen et al. [40] made a computational study on the effects of porosity on erosion behaviour of TiC/Cu composites in which they have demonstrated that the porosity could be often beneficial to the performance of the composites.

Metal Matrix composites are often used as engineering as well as structural components functioning in hostile workplaces where they are subjected to erosive wear situations. Solid particle erosion is to be expected whenever hard particles are entrained in a gas or liquid medium impinging on a solid at any significant velocity. In some cases solid particle erosion is a useful phenomenon,

as in sand-blasting and high-speed abrasive water jet cutting, but it is a serious problem in many engineering systems, including steam and jet turbines, pipelines and valves carrying particulate matter and fluidized bed combustion systems. It is a quite complex phenomenon, since it involves several processes. Although the main process is the mechanical impact, caused by the impingement of solid particles on the target material, secondary processes, like thermal, chemical and physical reactions between the counterparts take place during erosion. Studies to develop an understanding of the mechanisms of erosive wear have been motivated by reduced lifetimes and failures of components used in erosive environments, e.g. in pipelines carrying sand slurries, in petroleum refining, in gas turbine/compressor blades, in rocket motor tail-nozzles and in boiler tubes exposed to fly ash. Degradation of materials due to solid particle erosion, either at room temperature or at elevated temperature, is encountered in a large variety of engineering industries as illustrated in Table 2.3.

Systems	Components
Chemical plant	Transport tubes carrying abrasive materials in an air stream [89-91]
Hydraulic mining machinery	Pumps and valves [92]
Propellant system	Rocket motors trail nozzle, gun barrel [93]
Combustion system	Burner nozzle, reheater, super heater and economizer tube banks [94, 95]
Fluidized bed combustion	Boiler heat exchanger tubes in bed tubes, tube banks and expander turbine [94,96-98]
Coal gasification	Turbine, lock hopper valves [94]
Coal liquefaction	Valve to throttle the flow of product steam[94]
Aircraft engine	Compressor and turbine blades [99]
Helicopter engine	Rotor and gas turbine blades [100]

Table 2.3 Examples of components subjected to solid particle erosion

2.7 Implementation of Design-of-Experiments for Wear Analysis

Statistical methods have commonly been used for analysis, prediction and/or optimization of a number of engineering processes. Such methods enable the user to define and study the effect of every single condition possible in an

experiment where numerous factors are involved. Solid particle erosion is a complex wear phenomenon in which a number of control factors collectively determine the performance output i.e. the erosion rate and there is enormous scope in it for implementation of appropriate statistical techniques for process optimization. But unfortunately, such studies have not been adequately reported so far. The present work addresses to this aspect by adopting a systematic statistical approach called Taguchi method to optimize the process parameters leading to minimum erosion of the polymer composites under study.

Wear processes in composites are complex phenomena involving a number of operating variables and it is essential to understand how the wear characteristics of the composites are affected by different operating conditions. Although a large number of researchers have reported on properties, performance and on wear characteristics of composites, neither the optimization of wear processes nor the influence of process parameters on wear rate has adequately been studied yet. Selecting the correct operating conditions is always a major concern as traditional experiment design would require many experimental runs to achieve satisfactory result. In any process, the desired testing parameters are either determined based on experience or by use of a handbook. It, however, does not provide optimal testing parameters for a particular situation. Thus, several mathematical models based on statistical regression techniques have been constructed to select the proper testing conditions [101-106]. The number of runs required for full factorial design increases geometrically whereas fractional factorial design is efficient and significantly reduced the time. This method is popular because of its simplicity, but this very simplicity has led to unreliable results and inadequate conclusions. The fractional design might not contain the best design point. Moreover, the traditional multi-factorial experimental design is the *change one-factor-at-a-time* method. Under this method only one factor is varied, while all the other factors are kept fixed at a specific set of conditions.

To overcome these problems, Taguchi and Konishi [107] advocated the use of orthogonal arrays and Taguchi [108] devised a new experiment design that applied signal-to-noise ratio with orthogonal arrays to the robust design of products and processes. In this procedure, the effect of a factor is measured by average results and therefore, the experimental results can be reproducible. Phadke [109], Wu and Moore [110] and others [111, 112] have subsequently applied the Taguchi method to design the products and process parameters. This inexpensive and easy-to-operate experimental strategy based on Taguchi's parameter design has been adopted to study effect of various parameters and their interactions in a number of engineering processes.

2.8 Implementation of Artificial Neural Network for Wear Prediction

Wear process is considered as a non-linear problem with respect to its variables: either materials or operating conditions. To obtain minimum wear rate, combinations of operating parameters have to be planned. Therefore a robust methodology is needed to study these interrelated effects. In this work, a statistical method, responding to the constraints, is implemented to correlate the operating parameters. This methodology is based on ANN, which is a technique that involves database training to predict input-output evolutions.

The use of neural networks represents a new methodology in many different applications. It is a promising field of research in predicting experimental trends and has become increasingly popular in the last few years as they can often solve problems much faster compared to other approaches with the additional ability to learn. Generally, a neural network means a network of many simple processors ("units") operating in parallel, each possibly having a small amount of local memory. The units are connected by communication channels ("connections") which usually carry numeric (as opposed to symbolic) data, encoded by one of various ways [113]. One of the best known examples of a biological neural network is the human brain. It has the most complex and powerful structure which, by learning and training, controls human behaviour

towards responding to any problem encountered in every-day life. As for the artificial neural networks (ANN), they have been developed to emulate this biological network for the purpose of learning the solution to a physical problem from a given set of examples.

Back propagation algorithm can be used to train these multi-layer feed-forward networks with differentiable transfer functions to perform function approximation, pattern association, and pattern classification. In the vast majority of papers that deal with the prediction and forecasting of environmental variables, feed-forward networks optimized with the aid of the back-propagation algorithm (known as back-propagation networks) have been used [114]. The term back propagation refers to the process by which derivatives of network error, with respect to network weights and biases, can be computed. The training of an ANN by back propagation involves three stages: (a) the feed-forward of the input training pattern, (b) the calculation and back propagation of the associated error, and (c) the adjustment of the weights.

ANN can be customized and trained by using a certain amount of experimental data to a well designed ANN. After the network has learnt to solve the material problems, new data from the similar domain can then be predicted without performing too many long experiments [115]. The ANN method is suitable when (i) large database is available, (ii) it is difficult to find an accurate solution for a problem by mathematical approaches, (iii) the data set is incomplete, noisy and complex [116]. A 3 layered back-propagation network which is an effective tool to predict parameters with non-linear relationships could predict density, porosity, hardness, tensile strength, flexural strength, toughness, roughness of machined surface, flow stress and solid particle erosion with a reasonable accuracy [117]. Rashed et al. [118] applied ANN technique to study the effect of size and weight percent of SiC particulates, applied pressure and test temperature on the wear resistance of Al356-SiC MMCs and have shown that ANN is an effective tool in the prediction of the properties of MMCs.

2.9 The Knowledge Gap in Earlier Investigations

This literature review on particulate reinforced metal matrix composites reveals the following knowledge gap in the earlier investigations, based on which the objectives of the present research work can be set.

1. Though much work has been reported on various wear characteristics of metals, alloys and homogeneous materials, comparatively less has been reported on the erosive wear performance of metal matrix composite and their alloy elements.
2. A possibility that the incorporation of hard ceramic particles in MMCs could provide a synergism in terms of improved erosive wear resistance has not been adequately addressed so far and there is inadequate data available about phenomena behind the modified wear behaviour due to the addition of particulate fillers to the metal matrix composites.
3. Studies carried out worldwide on erosion behaviour of composites have largely been experimental and use of statistical techniques in analyzing wear characteristics is rare.
4. Taguchi method, in spite of being a simple, efficient and systematic approach to optimize designs for performance, quality and cost, is used only in a limited number of applications worldwide. Its implementation in parametric appraisal of wear processes has hardly been reported.
5. The use of prediction tools like artificial neural network (ANN) in order to predict wear rate of metal matrix composites is rarely reported.

2.10 Objectives of the Present Work

The objectives of this research work are outlined as follows:

1. Fabrication of a new class of ZA-27 based metal matrix composites reinforced with alumina and silicon carbide particles.
2. Physical and mechanical characterization of these composites.
3. Study of solid particle erosion wear characteristics of these ceramic particulate reinforced ZA-27 metal matrix composites under different test conditions.
4. Statistical analysis based on Taguchi experimental design for parametric appraisal of erosion wear process for the composites under study and development of predictive equations.
5. Implementation of artificial neural network for prediction of wear response of these composites under different operating conditions

Chapter Summary

This chapter has provided

- An exhaustive review of research works on various aspects of metal matrix composites reported by previous investigators.
- The knowledge gap in earlier investigations.
- The objectives of the present work.

The next chapter describes the materials and methods used for the processing of the composites, the experimental planning, Taguchi's method and artificial neural network technique.

Chapter 3

Experimental Details

EXPERIMENTAL DETAILS

This chapter describes the materials used for the fabrication of the metal matrix composites and the test methods employed to carry out this investigation. It presents the details of the tests related to the physical, mechanical, micro-structural and tribological characterization of the prepared MMC specimens. The methodology based on Taguchi experimental design and the prediction model inspired by artificial neural network are also described in this part of the thesis.

3.1 Materials

3.1.1 Matrix material

In the present study, Zinc-aluminium alloy i.e. ZA-27 is used as the matrix material. The chemical composition of this alloy according to ASTM B 669-82 ingot specification is shown in Table 3.1 and some of its main engineering properties are presented in Table 3.2. The key properties are higher tensile strength, fairly good thermal conductivity, lower specific weight and easy machinability. ZA-27 is the lightest alloy in the group of zinc-aluminium alloys and therefore it is widely used in bearings, automobile parts like clutches, brakes, connecting rods, exhaust valves etc. so as to increase the fuel efficiency of the vehicles. ZA-27 alloy also finds application in the core for power lines. Figure 3.1 illustrates few different forms of ZA-27 alloys available in the field of application.

Table 3.1: Chemical composition of ZA-27 alloy

Materials	Al	Cu	Mg	Zinc
Wt %	25-28	2-2.5	0.01-0.02	Balanced

Table 3.2 Engineering Properties of ZA-27alloy

Properties	Values	Units
Ultimate Tensile Strength	420-490	MPa.
Yield Strength	378	MPa.
Hardness	90-120	BHN
Density at 20° C.	4.7-4.9	gms/Cm ³
Solidification Temperature range	480-580	° C.
Thermal Conductivity at 20-100° C (x 10 ⁻⁶ .)	136	mm/mm/° C
Co-efficient of friction.	0.01-0.30	
Young's Modulus	77.9	GPa
Poisson ratio	0.32	

**Figure 3.1** Different forms of available ZA-27 alloys

3.1.2 Filler materials

The filler materials are generally discontinuous, stronger and harder than the matrix materials. The main function of these filler materials is to improve the physical, mechanical and tribological properties of the composite. These filler materials are of many types like long fibers, short fibers, whiskers and particulates types. Some commonly used fibers are glass fibers, bio fibers, silicon carbide fibers, graphite fibers etc. Some of the most commonly used particles are aluminum oxide (Al₂O₃), silicon carbide (SiC), graphite, garnet etc. In the present investigation, two most commonly used and easily available

ceramics particles (i.e. aluminum oxide and silicon carbide) are used as the filler materials to improve the mechanical and wear resistance properties of the ZA 27 alloy.

Filler Material – 1 (Al_2O_3)

Aluminium oxide, commonly referred to as alumina, is the most cost effective and widely used material in the family of engineering ceramics. With an excellent combination of properties and an attractive price, it is no surprise that fine grain technical grade alumina has a very wide range of applications. Its high hardness, excellent dielectric properties, refractoriness and good thermal properties make it the material of choice for a wide range of applications. Some typical uses of alumina are wear pads, seal rings, high temperature electrical insulators, furnace liner tubes, abrasion resistance tubes etc.

Key Properties

- ✓ Hard, wear-resistant
- ✓ Good thermal conductivity
- ✓ High strength and stiffness
- ✓ High working temperature



Figure 3.2 Commercially available alumina particles

Table 3.3 Engineering Properties of Aluminium Oxide

Properties	Values	Units
Density	3.89	gm/cc
Flexural Strength	379	MPa
Elastic Modulus	375	GPa
Shear Modulus	152	GPa
Bulk Modulus	228	GPa
Poisson's Ratio	0.22	----
Compressive Strength	2600	MPa
Hardness	1440	Kg/mm ²
Maximum Use Temperature	1750	°C
Thermal Conductivity	35	W/m°K
Coefficient of Thermal Expansion	8.4	10 ⁻⁶ /°C

Filler Material – 2 (SiC)

Silicon carbide is composed of tetrahedra of carbon and silicon atoms with strong bonds in the crystal lattice. This produces a very hard and strong material. Silicon carbide is not attacked by any acids or alkalis or molten salts up to 800°C. In air, SiC forms a protective silicon oxide coating at 1200°C and is able to be used up to 1600°C. The high thermal conductivity coupled with low thermal expansion and high strength gives this material exceptional thermal shock resistant qualities. Some typical uses of silicon carbide are found in fixed and moving turbine components, seals, bearings, heat exchangers etc.

Key Properties

- ✓ Low density
- ✓ High strength
- ✓ Low thermal expansion
- ✓ High hardness
- ✓ High elastic modulus
- ✓ Excellent thermal shock resistance



Figure 3.3 Commercially available silicon carbide particles

Table 3.4 Engineering Properties of Silicon Carbide

Properties	Values	Units
Density	3.1	gm/cc
Flexural Strength	550	MPa
Elastic Modulus	410	GPa
Poisson's Ratio	0.14	----
Compressive Strength	3900	MPa
Hardness	2800	Kg/mm ²
Maximum Use Temperature	1650	°C
Thermal Conductivity	120	W/m°K
Coefficient of Thermal Expansion	4.0	10 ⁻⁶ /°C

3.2 Phase Diagram of ZA-27 Alloy

Zinc-aluminium phase diagram is shown in Figure 3.4. This diagram shows that, ZA-27 while cooling from melt to room temperature, goes through several phases, namely (α +L), α' , (α + α') and finally (α + β).

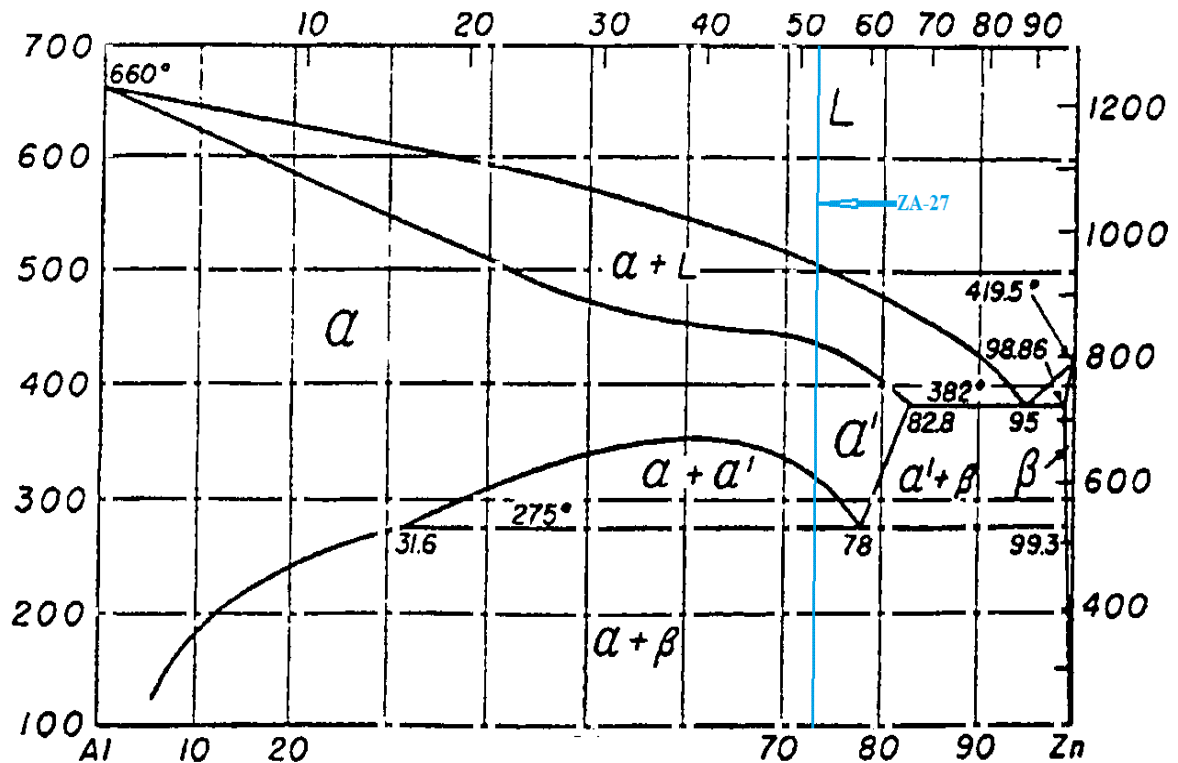


Figure 3.4 Phase diagram of Zinc-Aluminium alloy

3.3 Composite Fabrication

3.3.1 Techniques

The fabrication of the metal matrix composites are mainly based on two technological methods such as solid state processing and liquid state processing. In solid state processing, reinforcement are embedded in the matrix through diffusion phenomenon and are produced at high pressure and temperature. In this process, some special care should be taken to avoid the growth of undesirable phases or compounds species on interface. Some commonly used techniques under this method are diffusion bonding, powder metallurgy etc. In liquid state processing, the matrix is in liquid form and the reinforcement either in form of fibers or particles are embedded into it. The uniformity in distribution of reinforcement can be made by means of applying some mechanical actions. This is one of the most used and inexpensive method for fabrication of metal matrix composites. Hot forming, liquid infiltration, squeeze casting and stir casting are some common techniques under this method.

Among the variety of techniques available for fabrication of MMCs, stir casting is generally most simple, cost effective and accepted technique. In this method, after the matrix material is melted, it is stirred vigorously to form a vortex at the surface of the melt, and the reinforcement material is then introduced at the side of the vortex. The particles transfer into the matrix melt due to the pressure difference between the inner and the outer surface of the melt.

3.3.2 Procedure

In this process, melting of the matrix alloy ZA-27 is carried out separately about 800°C , above its melting temperature using muffle furnace. After melting, the required quantity of filler particulates (0, 3, 6 and 9 wt%), preheated to around 400°C , are added to the molten metal and stirred continuously by using a mechanical stirrer (Figure 3.5 a). The stirrer is rotated at a speed of 450 rpm for 2-3 min in order to get uniform mixing of filler particulate in the matrix material. During stirring, to enhance the wettability, small quantities of magnesium are added to the melt. The molten metal is then poured into permanent mould of cast iron of size $120 \times 30 \times 5 \text{ mm}^3$ (i.e. length \times width \times thickness) for casting and the temperature is then lowered gradually (Figure 3.5 b). After solidification, the castings are taken from the mold and are cut to the required shape and sizes ($30 \times 30 \times 5 \text{ mm}^3$) for erosion test.

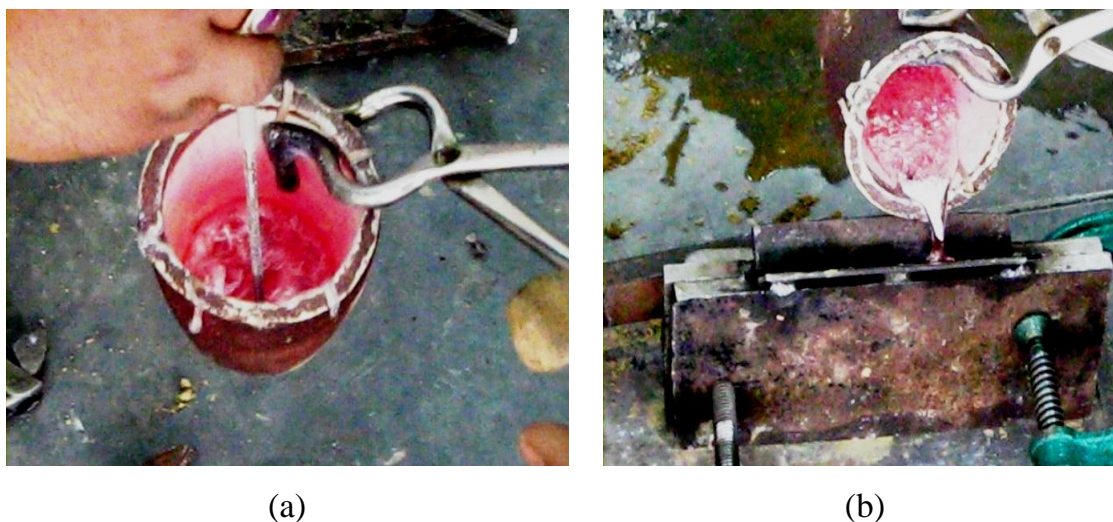


Figure 3.5 Composite fabrication steps (a-b)

3.4 Mechanical Characterization

3.4.1 Micro-hardness measurement

Micro-hardness measurement is done using a Leitz Micro-Hardness Tester (Figure 3.6). A diamond indenter, in the form of a right pyramid with a square base and an angle 136° between opposite faces, is forced into the material under a load F . The two diagonals X and Y of the indentation left on the surface of the material after removal of the load are measured and their arithmetic mean L is calculated. In the present study, the load considered is $F = 49.08$ N and Vickers hardness number is calculated using the following equation [119].

$$H_v = 0.1889 \frac{F}{L^2}$$

$$\text{and } L = \frac{X + Y}{2} \quad (3.3)$$

Where F is the applied load (N), L is the diagonal of square impression (mm), X is the horizontal length (mm) and Y is the vertical length (mm).

3.4.2 X-Ray Diffraction (XRD) Studies

The composite specimens with different fillers are examined for the identification of the crystalline phases with an X'Pert X-Ray Diffractometer (Figure 3.7). The X-ray diffractograms are taken using $\text{Cu K}\alpha$ radiation.

3.4.3 Tensile, flexural and impact strength measurement

The tensile test is generally performed on flat specimens. The commonly used specimens for tensile test are the dog-bone type and the straight side type with end tabs. During the test a uni-axial load is applied through both the ends of the specimen. The ASTM standard test method for tensile properties of metal matrix composites has the designation D3552/D3552M. The length of the test section should be 76 mm. The tensile test is performed in the universal testing machine (UTM) Instron 1195 (Figure 3.8) and results are analyzed to calculate the tensile strength of composite samples. The loading arrangement is shown in Figure 3.9.



Figure 3.6 Leitz Micro-hardness Tester



Figure 3.7 X'Pert X-Ray Diffractometer

The short beam shear (SBS) tests are performed on the composite samples at room temperature to evaluate the value of flexural strength. It is a 3-point bend test, which generally promotes failure by inter-laminar shear. The SBS test is conducted as per ASTM standard (D5379/D5379M) using the same UTM. The loading arrangement is shown in Figure 3.10. The flexural strength (*F.S.*) of any composite specimen is determined using the following equation.

$$F.S = \frac{3PL}{2bt^2} \quad (3.4)$$

Where, *L* is the span length of the sample.

P is the load applied;

b and *t* are the width and thickness of the specimen respectively.

The pendulum impact testing machine (ASTM D-256) ascertains the notch impact strength of the material by shattering the V-notched specimen with a pendulum hammer, measuring the spent energy and relating it to the cross section of the specimen. The machine is adjusted such that the blade on the free-hanging pendulum just barely contracts the specimen (zero position). The specimens are clamped in a square support and are struck at their central point by a hemispherical bolt of diameter 5 mm.

3.5 Scanning Electron Microscopy

The surfaces of the composite specimens are examined directly by scanning electron microscope JEOL JSM-6480LV (Figure 3.11). The specimens are cleaned thoroughly with acetone before being observed under SEM at 20 kV. Then the composite samples are mounted on stubs and the eroded and uneroded surfaces are examined.



Figure 3.8 Pictorial view of Universal Testing Machine Instron 1195



Figure 3.9 Loading arrangement for tensile test



Figure 3.10 Loading arrangement for three point bend test



Figure 3.11 Scanning Electron Microscope (JEOL JSM - 6480LV)

3.6 Tribological Characterization

3.6.1 Solid Particle Erosion Wear Test

The set up for the solid particle erosion wear test used in this study is capable of creating reproducible erosive situations for assessing erosion wear resistance of the prepared composite samples. The schematic diagram of the erosion test rig is given in Figure 3.12 and pictorial view is shown in Figure 3.13. The test rig consists of an air compressor, an air drying unit, a particle feeder and an air particle mixing and accelerating chamber.

In the present study, dry silica sand of average particle size of $450\mu\text{m}$ is used as erodent. The dried and compressed air is mixed with the erodent which is feed constantly by a particle feeder into the mixing chamber and then is accelerated by passing the mixture through a convergent tungsten carbide nozzle of 3 mm internal diameter. The erodent particles impact the specimen which can be held at different angles with respect to the direction of erodent flow and the stand-off-distance between the nozzle and the specimen surface can be control by using different holder and arrangement as shown in Figure 3.13. The velocity of the eroding particles is determined using the standard double disc method [119, 120].

The samples are cleaned in acetone, dried and weighed before and after the erosion trials using a precision electronic balance to an accuracy of ± 0.1 mg. The weight loss is recorded for subsequent calculation of erosion rate. The process is repeated till the erosion rate attains a constant value called *steady state erosion rate*. The ratio of this weight loss to the weight of the eroding particles causing the loss is then computed as the dimensionless incremental erosion rate. The erosion rate is defined as the weight loss of the specimen due to erosion divided by the weight of the erodent causing the loss.

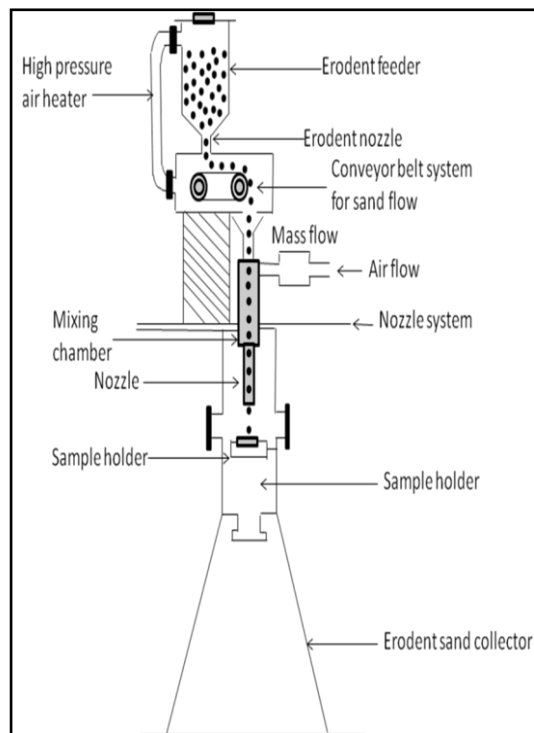


Figure 3.12 Schematic diagram of erosion test rig



Figure 3.13 Solid particle erosion trails set-up

3.7 Process Optimization and Taguchi Method

Statistical methods are commonly used to improve the quality of a product or a process. Such methods enable the user to define and study the effect of every single condition possible in an experiment where numerous factors are involved. Wear processes such as sliding and/or erosion are such processes in which a number of control factors collectively determine the performance output i.e. the wear rate. Hence, in the present work a statistical technique called Taguchi method is used to optimize the process parameters leading to minimum wear of the composites under study.

3.7.1 Taguchi Experimental Design

Every single discipline in engineering has researchers carrying out experiments to observe and understand a certain process or to discover the interaction and effect of different variables on the output. From a scientific viewpoint, these experiments are either one or a series of tests to either confirm a hypothesis or to understand a process in further detail. In order to achieve a meaningful end result, several experiments are usually carried out. The experimenter needs to know the factors involved, the range these factors are varied between, the levels assigned to each factor as well as a method to calculate and quantify the response of each factor. This *one-factor-at-a-time* approach will provide the most favorable level for each factor but not the optimum combination of all the interacting factors involved. Thus, experimentation in this scenario can be considered as an iterative process. Although it will provide a result, such methods are neither time nor cost effective. But the design-of-experiments (DOE) is a scientific approach to effectively plan and perform experiments using statistics. In such designs, the combination of each factor at every level is studied to determine the combination that would yield the best result. DOE in fact is a powerful analysis tool for modeling and analyzing the influence of control factors on performance output. The most important stage in the DOE lies in the selection of the control factors. Therefore, a large number of factors are initially included so that the less significant variables can be identified at the earliest opportunity.

Exhaustive literature review presented in the previous chapter reveals that as far as erosion wear is concerned, impact velocity, filler content, impingement angle, stand-off-distance, erodent temperature etc. largely influence the wear rate of metal matrix composites [30,33,75,82-85]. The impact of these five parameters on the erosion wear rate of these particulates filled ZA-27 metal matrix composites is therefore studied in this work using Taguchi's L_{16} orthogonal array design. The control factors and the parameter settings for erosion test are given in Table 3.5. Table 3.6 presents the selected levels for various control factors. The tests are conducted as per the L_{16} experimental design given in Table 3.7. As already mentioned, in a conventional full factorial design, it would normally require $4^5 = 1024$ runs to study five parameters each at four levels, whereas Taguchi's factorial experiment approach reduces it to only 16 runs, offering a great advantage in terms of experimental time and cost.

Table 3.5 Parameter settings for erosion test

Control Factors	Symbols	Fixed Parameters	
Impact velocity	A	Erodent	Silica sand
Filler content	B	Erodent feed frequency (HZ)	10.0±0.1
Impingement angle	C	Erodent size (µm)	240
Stand-off-distance	D	Nozzle diameter (mm)	3
Erodent temperature	E	Nozzle length (mm)	80

Table 3.6 Control factors and their selected levels (for erosion test)

Control Factor	Level				
	I	II	III	IV	Units
A: Impact Velocity	35	45	55	65	m/sec.
B: Filler Content	0	3	6	9	wt. %
C: Impingement angle	45	60	75	90	degree
D: Stand-off-distance	55	65	75	85	mm
E: Erodent temperature	35	70	105	140	⁰ C

The experimental observations are further transformed into signal-to-noise (S/N) ratios. There are several S/N ratios available depending on the type of characteristics as given by the Equations. 3.5, 3.6 and 3.7.

Table 3.7 Taguchi orthogonal array design (L₁₆) for solid particle erosion test

Test run	A (Impact velocity)	B (Stand-off-distance)	C (Erodent temperature)	D (Impingement angle)	E (Filler content)
1	1	1	1	1	1
2	1	2	2	2	2
3	1	3	3	3	3
4	1	4	4	4	4
5	2	1	2	3	4
6	2	2	1	4	3
7	2	3	4	1	2
8	2	4	3	2	1
9	3	1	3	4	2
10	3	2	4	3	1
11	3	3	1	2	4
12	3	4	2	1	3
13	4	1	4	2	3
14	4	2	3	1	4
15	4	3	2	4	1
16	4	4	1	3	2

‘Smaller- the- better’ characteristic: $S/N = -10 \log \frac{1}{n} \sum y^2$ (3.5)

‘Nominal- the- better’ characteristics: $S/N = -10 \log \left(\sum \frac{\bar{y}}{S^2} \right)$ (3.6)

‘Larger- the- better’ characteristics: $S/N = -10 \log \frac{1}{n} \left(\sum \frac{1}{y^2} \right)$ (3.7)

where n the number of observations and y the observed data. The S/N ratio for minimum wear rate comes under ‘smaller is better’ characteristic, which can be calculated as logarithmic transformation of the loss function by using Equation (3.5).

3.8 Neural Network Analysis

Erosion wear process is considered as a non-linear problem with respect to its variables: either materials or operating conditions. As already mentioned, to obtain minimum wear rate, appropriate combinations of operating parameters have to be planned so as to study their interrelated effects and to predict the wear response under different operational conditions. To this end, a systematic analysis using another novel technique namely artificial neural network (ANN) is implemented in this work. ANN is a technique inspired by the biological neural system and has already been used to solve a wide variety of problems in diverse fields [115, 122, 123]. It was developed to simulate the strong learning, clustering and reasoning capacity of the biological neurons. With a strong learning capability and use of parallel computation and nonlinear mapping, neural networks can be successfully applied for identifying several nonlinear systems and control problems. The multiple layered ANN is the most extensively applied neural network for various engineering materials. Using a well-trained ANN model, one can estimate predictive performance, pattern association and pattern classification. As aforementioned, the wear process is a complicated phenomenon lacking adequate mathematical description and therefore, a powerful method that combines the ANN technique and the Taguchi's design is proposed in this study for better analysis and prediction of wear performance of composites. This proposed approach not only yields a sufficient understanding of the effects of process parameters, but also produces an optimal parameter setting to ensure that the composites exhibit the best performance characteristics.

ANN is a technique that involves database training to predict input-output evolutions. Basically, this technology is suitable for some complex, non-linear and multi-dimensional problems because it is able to imitate the learning capability of human beings. This means the network can learn directly from the examples without any prior formulae about the nature of the problem and generate by itself some knowledge, which could be applied for new cases. A

neural network is a system composed of many cross-linked simple processing units called neurons. The network generally consists of three parts connected in series: input layer, hidden layer and output layer. The neurons or units of the network are connected by the weights. The coarse information is accepted by the input layer and processed in the hidden layer. Finally the results are exported via the output layer [124]. Figure 3.14 gives a schematic description of an ANN structure, as well as the network configuration. Back propagation (BP), which is one of the most famous training algorithms for multilayer perceptions, is a gradient descent technique to minimize the error for particular training pattern [125]. Experimental result sets are used to train the ANN in order to understand the input-output correlations. The database is divided into three categories, namely: (i) a validation category, which is required to define the ANN architecture and adjust the number of neurons for each layer. (ii) a training category, which is exclusively used to adjust the network weights and (iii) a test category, which corresponds to the set that validates the results of the training protocol.

Each input neuron of the input layer receives input signal X_i and broadcasts this signal to all neurons in the hidden layer. Each hidden neuron Y_j sums its weighted input signal and applies its transfer function to compute output signal.

$$Y_j = f\left(\sum_{i=1}^n W_{ij} X_i\right) \quad (3.8)$$

where W_{ij} is the weight from the input neuron X_i to the hidden neuron Y_j .

The output signal of the hidden neuron Y_j is sent to all neurons in the output layer. Each output neuron O_k sums its weighted input signal and applies its transfer function to compute its output signal.

$$O_k = f\left(\sum_{j=1}^n W_{jk} Y_j\right) \quad (3.9)$$

where W_{jk} is the weight from the hidden neuron Y_j to the output neuron O_k .

The transfer function used in this study is a logistic sigmoid function defined as:

$$f(x) = \frac{1}{1 + e^{-x}} \quad (3.10)$$

The BP training algorithm is an iterative gradient descent algorithm, designed to minimize the sum of square error (E) which is averaged all patterns is calculated as follows:

$$E = \frac{1}{2} \sum_{i=1}^p p_i - a_i \quad (3.11)$$

Where p_i the predicted output value, a_i is the actual output value for the i th pattern.

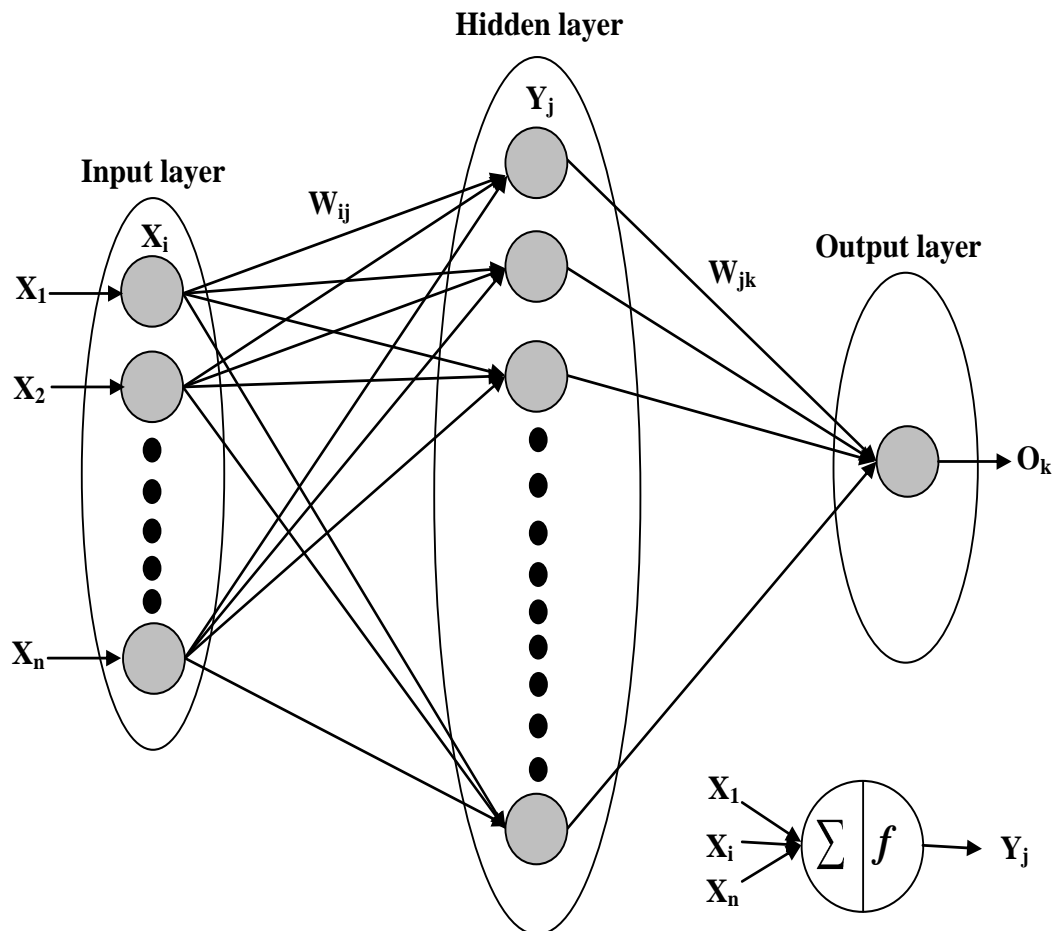


Figure 3.14 Line diagram of artificial neural network system

In the minimization process, the weights of all the connecting nodes are adjusted until the desired error level is achieved or the maximum cycle is reached. The error is minimized by adjustments of the weights according to the following mathematical equation:

$$\Delta W_{ji} = -\beta \partial E / \partial W_{ji} \quad (3.12)$$

where β is learning rate.

Training is the act of continuously adjusting the connection weights until they reach unique values that allow the network to produce outputs that are close enough to the actual desired outputs. The accuracy of the developed model, therefore, depends on these weights. Once optimum weights are reached, the weights and biased values encode the network's state of knowledge [126].

Chapter Summary

This chapter has provided:

1. The description of the materials used in the experiments.
2. The details of fabrication and characterization of the composites.
3. The description of solid particle erosion test.
4. An explanation of the Taguchi technique and neural computation.

The next chapter presents the physical and mechanical characterization of the particulate filled ZA-27 metal matrix composites under this investigation.

Chapter 4

Results and Discussion: Part-1

**Physical and Mechanical Characterization of the
Particulate Filled ZA-27 Metal Matrix Composites**

RESULTS AND DISCUSSION: PART-1

Physical and Mechanical Characterization of the Particulate Filled ZA-27 Metal Matrix Composites

This chapter presents the measured values of the physical and mechanical properties of the ZA-27 metal matrix composites reinforced with different ceramic particulate fillers. The results obtained for ZA-27 metal matrix composites reinforced with alumina and silicon carbide are compared. The relative effects of different filler materials on various properties of the composites have also been discussed.

4.1 Physical Characterization of the Composites

4.1.1 Density and Void Fraction

In many real time applications, metal matrix composites are found to replace conventional metals and materials primarily for their low densities. Density is a material property which is of prime importance in several weight sensitive applications. It depends on the relative proportion of matrix and the reinforcing materials in the composite. There is always a difference between the measured and the theoretical density values of a composite due to the presence of voids and pores. These voids significantly affect some of the mechanical properties and even the performance of composites. Higher void contents usually mean lower fatigue resistance, greater susceptibility to water penetration and weathering. The knowledge of void content is desirable for estimation of the quality of the composites.

In the present research work, the measured densities and volume fraction of voids (porosities) of all $\text{Al}_2\text{O}_3/\text{ZA-27}$ and $\text{SiC}/\text{ZA-27}$ metal matrix composites are presented in Table 4.1.

Measurement of porosity is done using the image analysis technique. The polished top coats are kept under a microscope (Neomate) equipped with a CCD camera (JVC, TK 870E). This system is used to obtain a digitized image of the object. The digitized image is transmitted to a computer equipped with VOIS image analysis software. The total area captured by the objective of the microscope or a fraction thereof can be accurately measured by the software. Hence the total area and the area covered by the pores are separately measured and the porosity of the surface under examination is determined.

Sample	Composition	Density (gm/cc)	Porosity (%)
01	ZA-27 alloy	3.8099	0.809
02	ZA-27+ 3wt% Al ₂ O ₃	3.9388	0.998
03	ZA-27+ 6wt% Al ₂ O ₃	4.0377	1.237
04	ZA-27+ 9wt% Al ₂ O ₃	4.1030	1.403
05	ZA-27+ 3wt% SiC	4.0665	1.065
06	ZA-27+ 6wt% SiC	4.3340	1.740
07	ZA-27+ 9wt% SiC	4.5884	2.188

Table 4.1 Measured densities along with the porosity

Sample	Composition	Micro-hardness (Hv)	Tensile strength (MPa)	Flexural strength (MPa)	Impact strength (J)
01	ZA-27 alloy	121.500	412	493	37
02	ZA-27+ 3wt% Al ₂ O ₃	124.125	417	483	39.8
03	ZA-27+ 6wt% Al ₂ O ₃	127.301	424	470	49.5
04	ZA-27+ 9wt% Al ₂ O ₃	130.258	430	432	57.6
05	ZA-27+ 3wt% SiC	135.210	429	387	43
06	ZA-27+ 6wt% SiC	138.258	438	375	51.5
07	ZA-27+ 9wt% SiC	142.563	447	368	59.3

Table 4.2 Mechanical properties of the composites

4.2 Mechanical Characterization of the Composites

A wealth of property data has been generated by conducting different characterization tests under controlled laboratory conditions to evaluate various mechanical characteristics of the composites fabricated for this work. The property values are presented in Table 4.2.

4.2.1 Micro-hardness

Hardness is considered as one of the most important factors that govern the wear resistance of any material. In the present work, micro-hardness values of the ZA-27 metal matrix composites (with and without particulate fillers) have been obtained by a Leitz micro-hardness tester. The variation of micro-hardness with different filler content in the composites is shown in Figure 4.1 and 4.2.

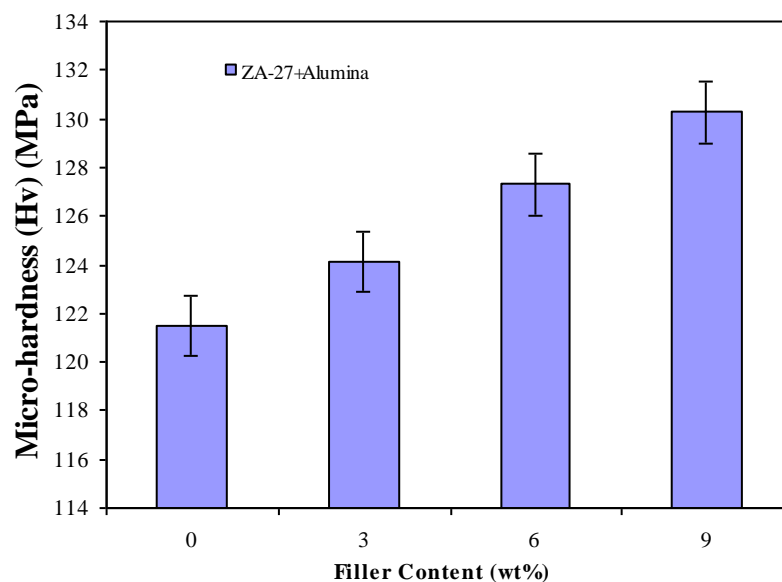


Figure 4.1 Variation of composite micro-hardness with alumina content

Among all the composites under this investigation, the maximum hardness value is observed for ZA-27 filled with 9 wt.% of SiC. The test results show that with the presence of hard ceramic particles, micro-hardness of the ZA-27 metal matrix composites improved from 121.5 Hv to 130.256 Hv for Al_2O_3 filled and to 142.563 Hv for SiC filled ZA-27 metal matrix composites. This implies an

increment of 7% and 17% in hardness for Al_2O_3 and SiC filled ZA-27 MMCs respectively.

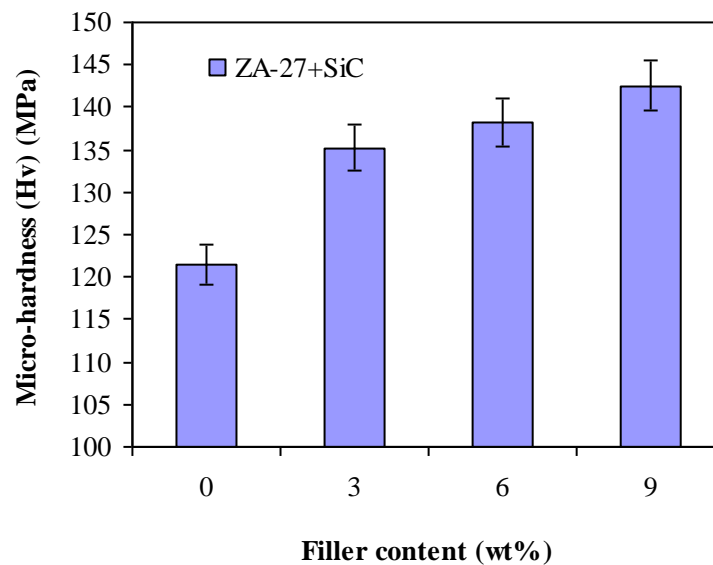


Figure 4.2 Variation of composite micro-hardness with silicon carbide content

4.2.2 Tensile strength

The test results for tensile strengths of the composites with Al_2O_3 and SiC are shown in Figures 4.3 and 4.4 respectively. It is seen that in all the samples, irrespective of the filler material the tensile strength of the composite increases with increase in filler content. The unfilled ZA-27 metal matrix composite has a strength of 412 MPa in tension and it may be seen from Table 4.2 that this value improves to 430 MPa with addition of 9 wt% of Al_2O_3 . In the case of SiC filled ZA-27 this improvement is found to be from 412 MPa to 447 MPa. The enhancement of tensile strength with incorporation of particulate fillers can be explained as follows. With the presence of hard particulates, the load on the matrix gets transferred to the reinforcing elements thereby increasing the load bearing capability of the composites. With increase in volume fraction of the filler material, more load gets transferred to reinforcement which leads to increase in tensile strength. Moreover, with the presence of hard ceramics like Al_2O_3 and SiC, there is a restriction to the plastic flow as a result of dispersion of

these hard particles in the matrix, thereby providing enhanced tensile strength in the composite.

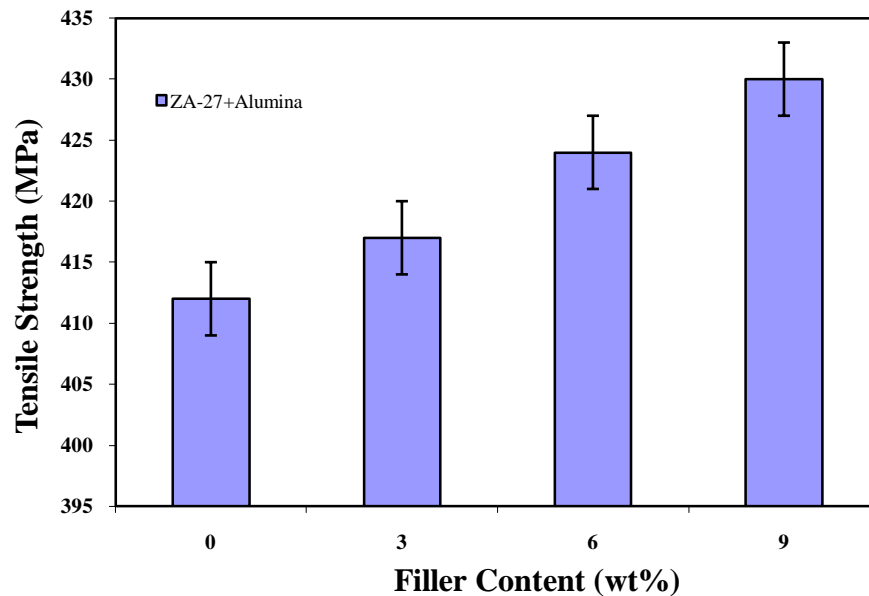


Figure 4.3 Variation of composite tensile strength with alumina content

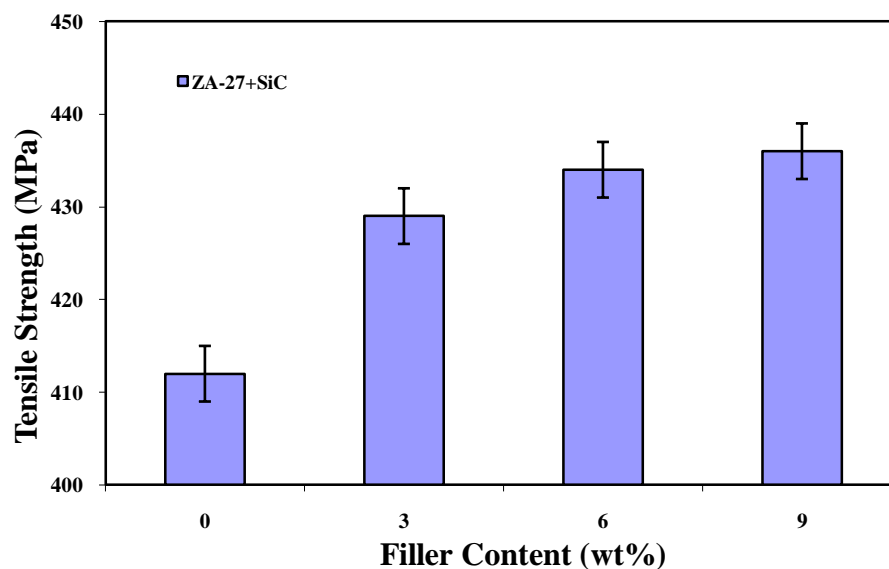


Figure 4.4 Variation of composite tensile strength with silicon carbide content

4.2.3 Flexural strength

Composite materials used in structures are prone to fail in bending and therefore the development of new composites with improved flexural characteristics is essential. In the present work, the variations of flexural strength of the ZA-27

metal matrix composites filled with alumina and silicon carbide particles are presented in Figure 4.5 and 4.6 respectively. Marginal decrement in flexural strength is recorded for all the composite samples with the incorporation of ceramic particles irrespective of the type of reinforcement.

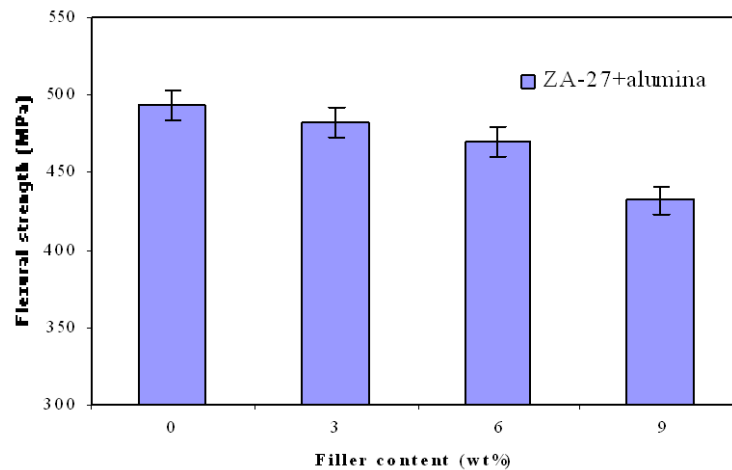


Figure 4.5 Variation of composite flexural strength with alumina content

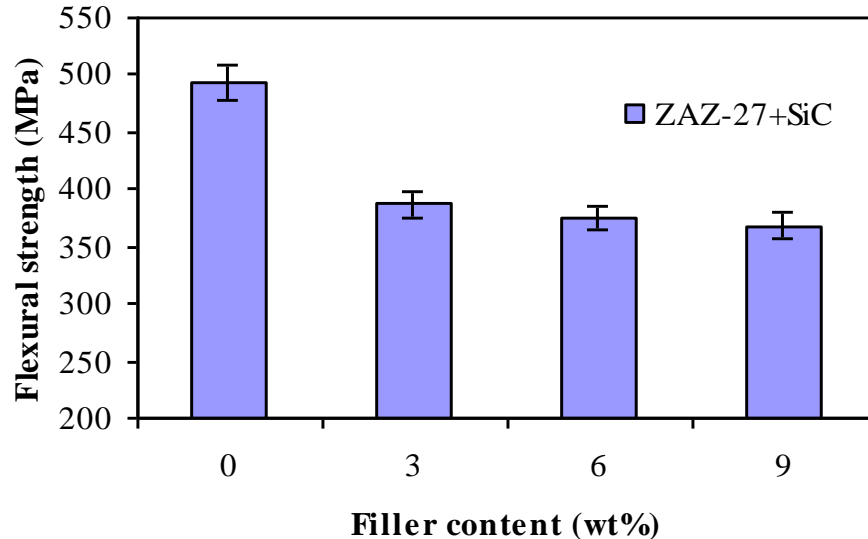


Figure 4.6 Variation of composite flexural strength with silicon carbide content

4.2.5 Impact strength

The impact strength of a material is its capacity to absorb and dissipate energies under impact or shock loading. The suitability of a composite for certain

applications is determined not only by usual design parameters, but also by its impact or energy absorbing properties. Thus, it is important to have a good understanding of the impact behaviour of composites for both safe and efficient design of structures.

Figures 4.7 and 4.8 present the measured impact energy values of the ZA-27 metal matrix composites filled with Al_2O_3 and SiC particulate fillers respectively. It is seen from both the figures that the impact energies of the composites increase gradually with filler content increasing from 3 to 9 wt%.

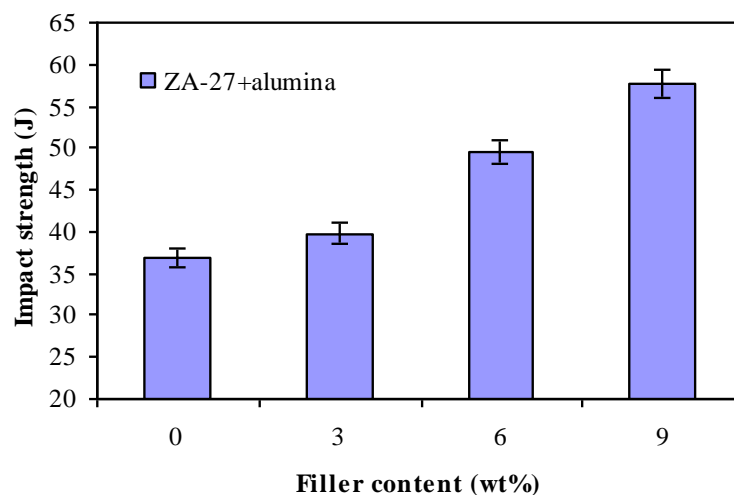


Figure 4.7 Variation of composite impact strength with alumina content

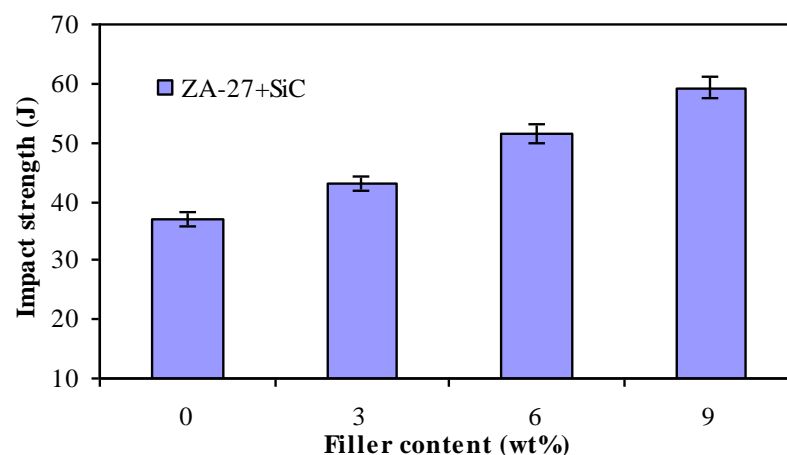


Figure 4.8 Variation of composite impact strength with silicon carbide content

4.3 X-Ray Diffraction (XRD) analysis

The chemical composition analysis of the ZA-27 alloy suggests that its major constituents are 25-28 wt% of Al, 2-2.5 wt% of Cu, 0.01-0.02 wt% of Mg and rest Zn. To ascertain the various phases present in the ZA-27 alloy and its composites, the X-ray diffractogram is taken and is shown in Figure 4.9, 4.10 and 4.11. It exhibits distinct peaks which are assignable to various phases such as Zn (101), Al (530, 532), Cu (311) and Mg (235). Distinct peaks for Al_2O_3 (211, 311) and SiC (210) in ZA-27 composites are also present in Figure 4.10 and 4.11 respectively.

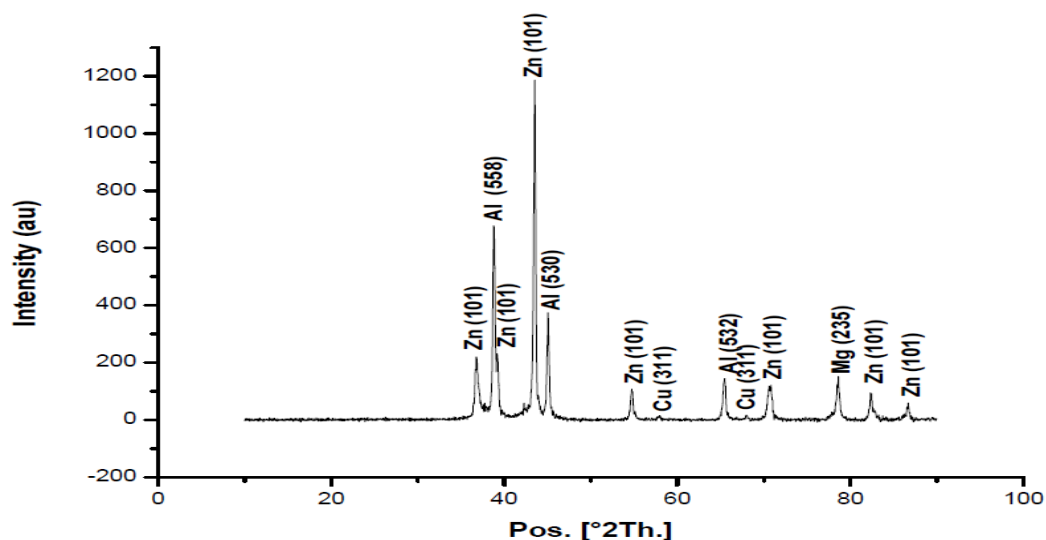


Figure 4.9 X-ray diffractogram of the ZA-27 alloy

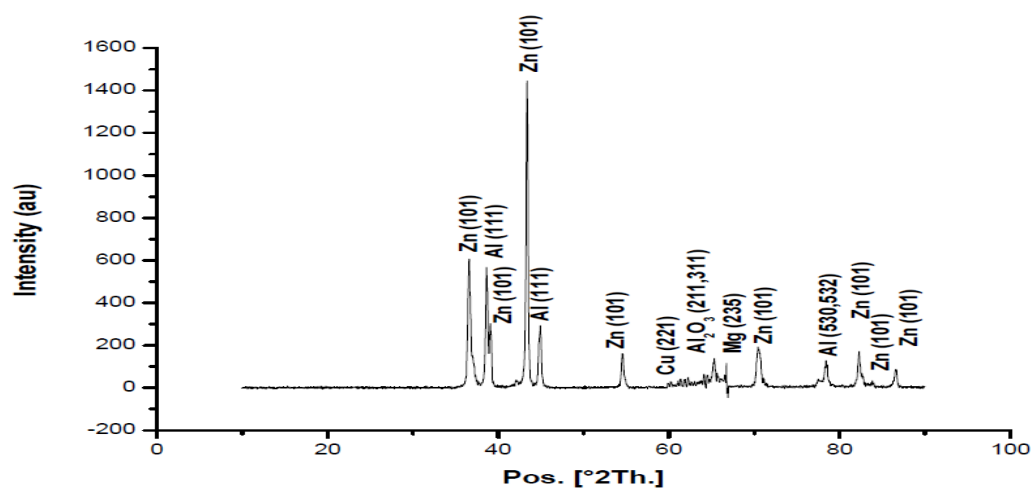


Figure 4.10 X-ray diffractogram of the Al_2O_3 filled ZA-27 MMC

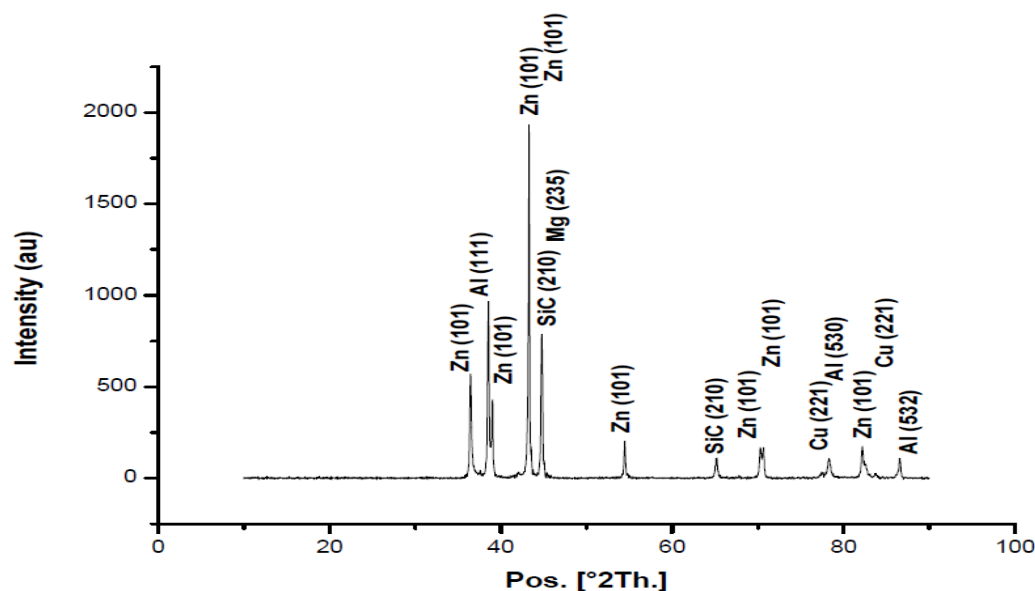


Figure 4.11 X-ray diffractogram of the SiC filled ZA-27 MMCs

Chapter summary

This chapter summarizes that:

- Successful fabrication of particulate (Al_2O_3 and SiC) filled ZA27 metal matrix composites is possible by stir casting route.
- Incorporation of these fillers modifies the tensile, flexural and impact strength of the ZA-27 metal matrix composites.
- The micro-hardness, density and porosity of the composites are also greatly influenced by the type and content of fillers.

The next chapter presents the experimental findings related to erosion wear characteristics of Al₂O₃/ZA-27 metal matrix composites.

Chapter 5

Results and Discussion: Part- 2

**Erosion Wear Characteristics of Al_2O_3 / ZA-27
Metal Matrix Composites**

RESULTS AND DISCUSSION (PART- 2)

Erosion Wear Characteristics of Al₂O₃ / ZA-27 Metal Matrix Composites

This chapter presents the results related to the erosion response of the ZA-27 metal matrix composites filled with Al₂O₃ particles. The solid particle erosion wear trials on these composites have been carried out following Taguchi experimental design (L₁₆ orthogonal array) given in Table 3.7. The micro-structural features as observed in the SEM images of the composite samples eroded under different operating conditions are described. Besides, the critical parametric analysis of the test results using Taguchi method and simulated wear predictions using artificial neural network model are presented.

5.1 Morphology of Eroded Composite Surfaces

The SEM micrographs of the uneroded and eroded surfaces of the ZA27 metal matrix composites under this study filled with alumina particles are presented in Figure 5.1. The micrograph in Figure 5.1a shows the surface of the composite filled with 9 wt% Al₂O₃. The surface appears to be smooth with no trace of wear. The SEM images in remaining (Figures 5.1 b-d) exhibit several forms of erosion and material removal process. The micrograph in Figure 5.1b reveals the initiation of chipping off of the composite surface due to repeated impact of hard silica sand particles. Figures 5.1c and 5.1d indicate plastic flow of matrix material along the erosion direction for the composite eroded at lower impact angle ($\alpha = 45^\circ$). When impacting at such low angle, the hard erodent particles penetrate the surface and cause material removal mostly by micro-ploughing. Once a particle has been removed, it forms a passage on the surface of the matrix, resulting in more efficient removal of matrix material. With increase in impact angle the pulling out of the Al₂O₃ particles is restricted. This is because

the impact is directly on the filler particles (Al_2O_3) whose hardness is much higher than the matrix materials leading to lower erosion. At oblique angles the removal of the matrix material took place more easily due to which the Al_2O_3 particles were exposed and after withstanding the impact for some time detached from the bond.

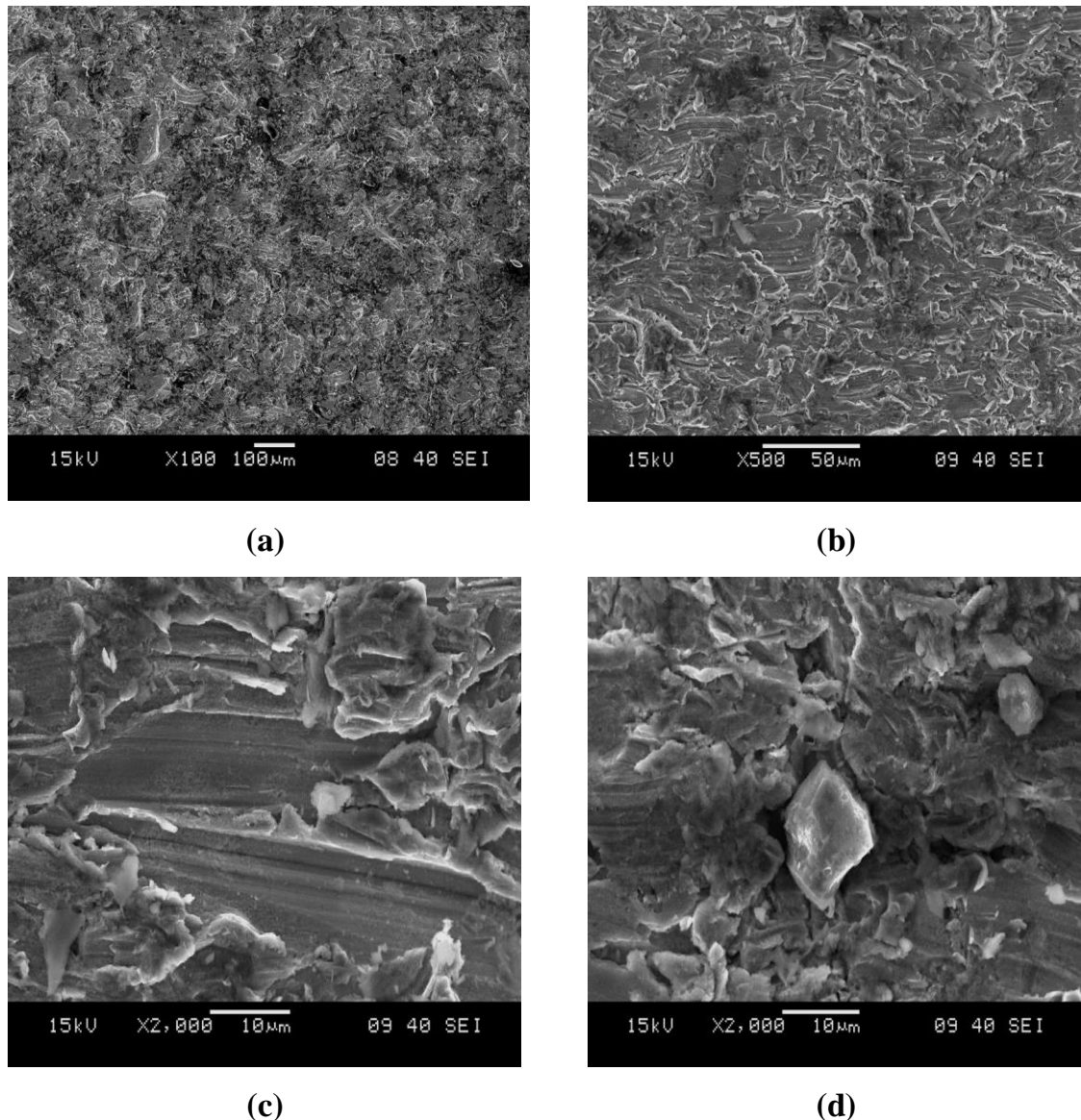


Fig. 5.1 SEM micrographs of the uneroded and eroded surfaces of the ZA27 metal matrix composites filled with 9 wt% Al_2O_3

5.2 Erosion Test Results and Taguchi Analysis

The erosion wear rates of Al_2O_3 reinforced ZA-27 metal matrix composites under various test conditions are given in Table 5.1. The difference between the weights of the composite before and after the erosion test is the *wear loss* or the mass loss of the specimen due to solid particle impact. The ratio of this mass loss to the mass of the eroding particles causing the loss is then computed as the dimensionless incremental erosion rate. The erosion rate is thus defined as the mass loss of the specimen due to erosion divided by the mass of the erodent causing the loss. Three samples are run for each combination of the test parameters employed and the results reported are the average of the three readings.

The experimental observations are then transformed into signal-to-noise (S/N) ratios. In the Table 5.1, the last column represents S/N ratio of the erosion rate which is in fact the average of three replications. There are several S/N ratios available depending on the type of characteristics. The S/N ratio for minimum erosion rate coming under *smaller-is-better* characteristic can be calculated as logarithmic transformation of the loss function as shown below:

$$S/N = -10 \log \frac{1}{n} \sum y^2 \quad (5.1)$$

where, n the number of observations and

y the observed data.

The overall mean for the S/N ratio of the erosion rate is found to be – 43.6992 dB. The analysis is made using the popular software specifically used for design of experiment applications known as MINITAB 14. Figure 5.2 shows graphically the effect of the five control factors on the erosion wear rate.

Test Run	Impact Velocity (A) m/sec	Stand-off distance (B) mm	Erodent temp. (C) °C	Impingement angle (D) degree	Filler content (E) wt %	Erosion rate (Er) mg/kg	Signal to noise ratio (S/N) db
1	35	55	35	45	0	145.667	-43.2672
2	35	65	70	60	3	101.287	-40.1111
3	35	75	105	75	6	80.924	-38.1615
4	35	85	140	90	9	72.500	-37.2068
5	45	55	70	75	9	125.001	-41.9383
6	45	65	35	90	6	143.693	-43.1487
7	45	75	140	45	3	182.572	-45.2287
8	45	85	105	60	0	194.888	-45.7957
9	55	55	105	90	3	199.287	-45.9896
10	55	65	140	75	0	221.333	-46.9009
11	55	75	35	60	9	112.500	-41.0231
12	55	85	70	45	6	145.615	-43.2641
13	65	55	140	60	6	249.998	-47.9587
14	65	65	105	45	9	160.834	-44.1276
15	65	75	70	90	0	243.333	-47.7240
16	65	85	35	75	3	232.858	-47.3418

Table 5.1 Erosion wear test results with the corresponding S/N ratios

Level	A	B	C	D	E
1	-39.69	-44.79	-43.70	-43.97	-45.92
2	-44.03	-43.57	-43.26	-43.72	-44.67
3	-44.29	-43.03	-43.52	-43.59	-43.13
4	-46.79	-43.40	-44.32	-43.52	-41.07
Delta	7.10	1.75	1.06	0.45	4.85
Rank	1	3	4	5	2

Table 5.2 Response table for signal to noise ratios

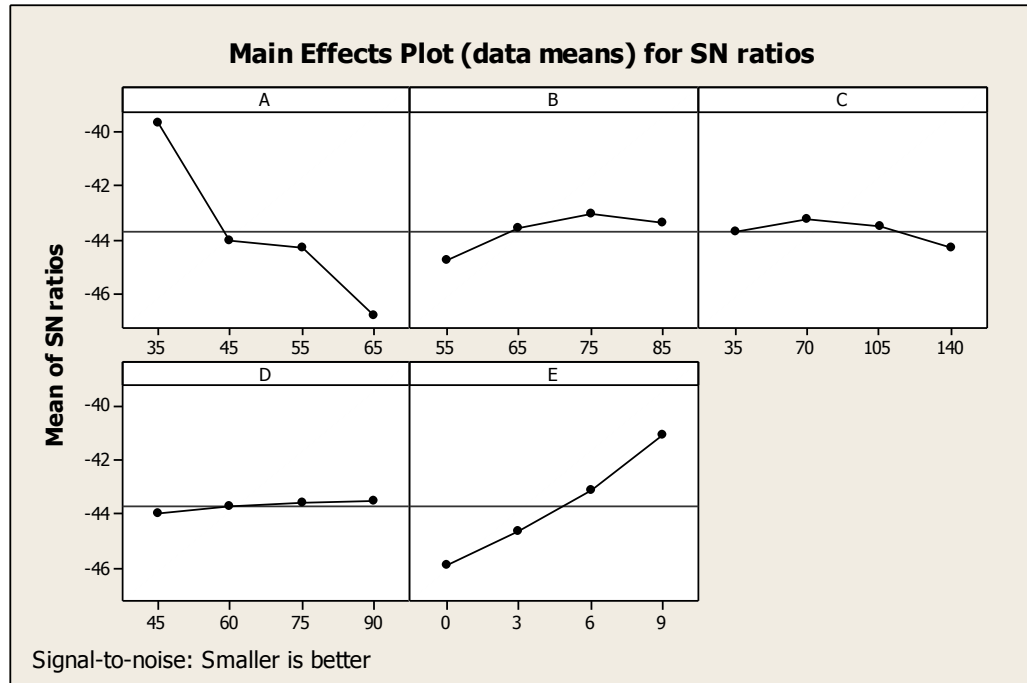


Figure 5.2 Effect of control factors on erosion rate

The S/N ratio response is given in the Table 5.2, from which it can be concluded that among all the factors, impact velocity is the most significant factor followed by filler content, stand-off-distance and erodent temperature while the impingement angle has least or negligible significance on erosion rate of these Al_2O_3 filled ZA-27 metal matrix composites. It also leads to the conclusion that factor combination of A1, B3, C2, D4 and E4 gives minimum erosion wear rate.

5.3 Factor Settings for Minimum Erosion Rate

In this study, an attempt is made to derive optimal settings of the control factors for minimization of erosion rate and a predictive equation is developed for determination of erosion rate in terms of the four most influential control factors. The single-objective optimization requires quantitative determination of the relationship between erosion rates with combination of control factors. In order to express, erosion rate in the form of a mathematical model, the following correlation is suggested.

$$E_r = K_0 + K_1 \times A + K_2 \times B + K_3 \times C + K_4 \times E \quad (5.2)$$

Here, E_r is the performance output term i.e. the erosion rate in mg/kg and K_i ($i = 0, 1, 2, 3, 4$) are the model constants. A is the impact velocity (m/s), B is the stand-off-distance (mm), C is the erodent temperature ($^{\circ}\text{C}$) and E is the filler content (wt.%). The constants are calculated using non-linear regression analysis with the help of SYSTAT 7 software and the following relations are obtained.

$$E_r = 39.696 + 3.731 \times A - 0.575 \times B + 0.211 \times C - 9.158 \times E \quad (5.3)$$

A comparison between experimental values and values obtained using this predictive equation for erosion rate along with corresponding percentage errors are given in Table 5.3. It is noted that the errors associated with the predictive values in regard to the experimental ones lie between 0 - 18% for most of the test runs. The correctness of the calculated constants is also confirmed as a high correlation coefficient (r^2) in the tune of 0.992 is obtained for Equation 5.2 and therefore, the model is quite suitable to be used for further predictive purpose.

Sl. No	Erosion Rate (mg/kg)		
	<i>Results obtain from predictive equation</i>	<i>Results obtain from experiment</i>	<i>Percentage error</i>
1	146.041	145.667	0.25675
2	120.202	101.287	18.67466
3	94.363	80.924	16.60694
4	68.524	72.500	5.48414
5	108.314	125.001	13.3495
6	122.653	143.693	14.6423
7	166.532	182.572	8.78558
8	180.871	194.888	7.19234
9	207.957	199.287	4.35051
10	237.066	221.333	7.108294
11	126.739	112.500	12.65689
12	155.848	145.615	7.027435
13	225.178	249.998	9.92808
14	184.569	160.834	14.75745
15	253.856	243.333	4.324526
16	213.247	232.858	8.42187

Table 5.3 Comparison of the experimental and the predictive erosion rates

5.4 Analysis and Prediction of Erosion Response using ANN

As mentioned earlier, artificial neural network (ANN) is a technique that involves database training to predict input-output evolutions. In this attempt to simulate the erosion wear process and to predict the erosion rate under different operating conditions for $\text{Al}_2\text{O}_3/\text{ZA-27}$ metal matrix composites, different ANN structures are tested and based on least error criterion, one structure is selected for training of the input-output data which is presented in Table 5.4. The optimized three layer neural network used in this simulation is shown in Figure 5.3

Input parameter for training	Values
Error tolerance	0.003
Learning parameter (β)	0.002
Momentum Parameter (α)	0.002
Noise Factor (NF)	0.001
Number of iteration	10, 000, 000
Slope parameter (ξ)	0.6
Number of layers	3
Number of neurons in input layer (I)	4
Number of neurons in hidden layer (H)	8
Number of neurons in output layer (O)	1

Table 5.4 Input parameters selected for training

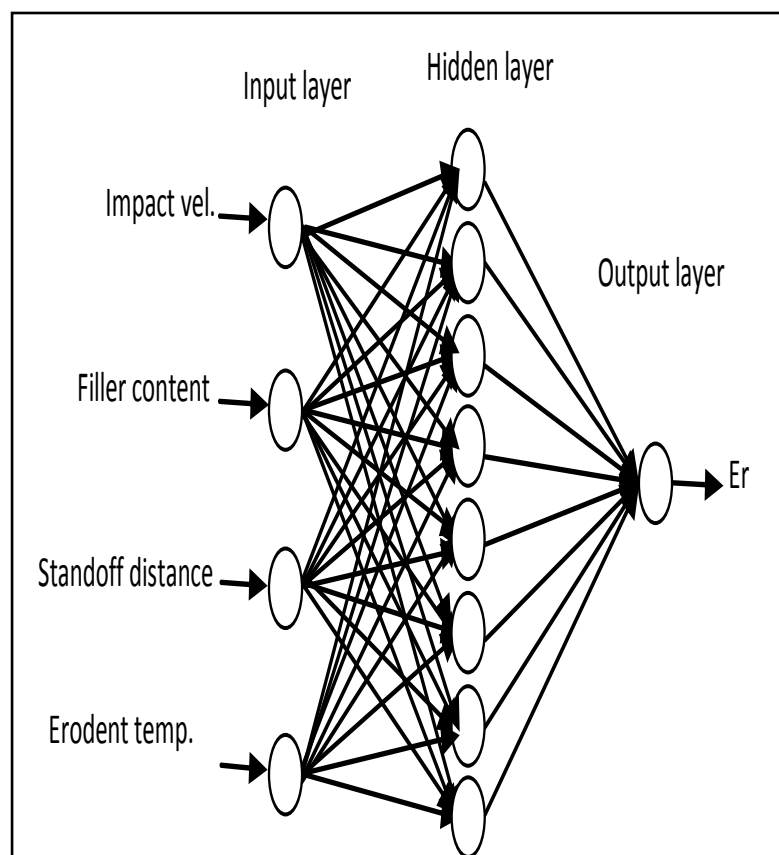


Figure 5.3 The three-layer neural network.

Erosion Rate (mg/kg) Experimental	Erosion Rate (mg/kg) ANN Prediction	Error Percentage (%)
145.667	141.959	2.54553
101.287	112.336	13.78154
80.924	85.464	5.610202
72.5	62.084	14.3669
125.001	124.167	0.66719
143.698	126.43	12.0169
182.572	166.341	8.89019
194.888	193.22	0.85588
199.287	223.087	11.94258
221.333	223.973	1.192773
112.5	112.313	0.16622
145.615	145.498	0.08035
249.998	242.011	3.19483
160.834	166.969	3.814492
243.333	253.854	4.323705
232.858	238.499	2.422506

Table 5.5 Comparison of the experimental and the ANN predicted erosion rates under similar test conditions

The ANN predictive results of erosion wear rate for all the 16 test conditions are shown and compared with the experimental values along with the associated percentage errors in Table 5.5. It is observed that the errors lie in the range of 0-14% which establishes the validity of the neural computation. The errors, however, can still be reduced and the quality of predictions can be further improved by enlarging the datasets and by optimizing the construction of the neural network. A well-trained ANN is expected to be very helpful for the analysis of erosion wear characteristics of any given composite and permits to study quantitatively the effect of each of the considered input parameters on the wear rate. The range of any chosen parameter can be beyond the actual experimental limits, thus offering the possibility to use the generalization property of ANN in a large parameter space. In the present investigation, this possibility has been explored by selecting the significant factors i.e. the impact velocity and filler content in a range wider than that of the experimental domain. Sets of predictions for erosion rate of $\text{Al}_2\text{O}_3/\text{ZA-27}$ metal matrix composites of different filler content are evolved and these predicted evolutions are illustrated in Figures 5.4, 5.5 and 5.6.

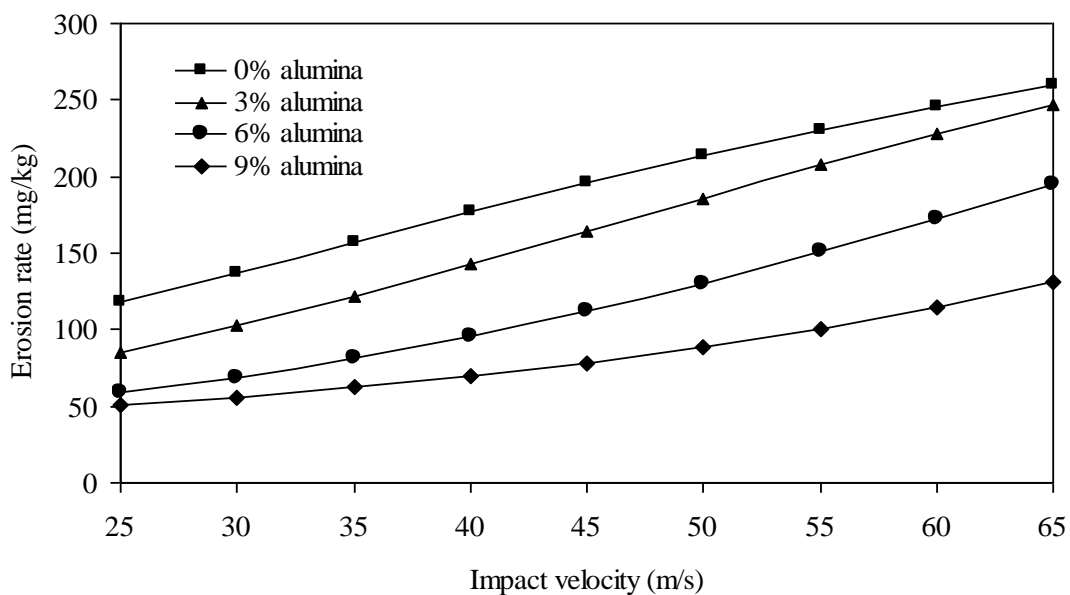


Figure 5.4 Predicted evolution of erosion rate of $\text{Al}_2\text{O}_3/\text{ZA-27}$ metal matrix composites with impact velocity (at stand-off-distance 55 mm and erodent temperature 140°C)

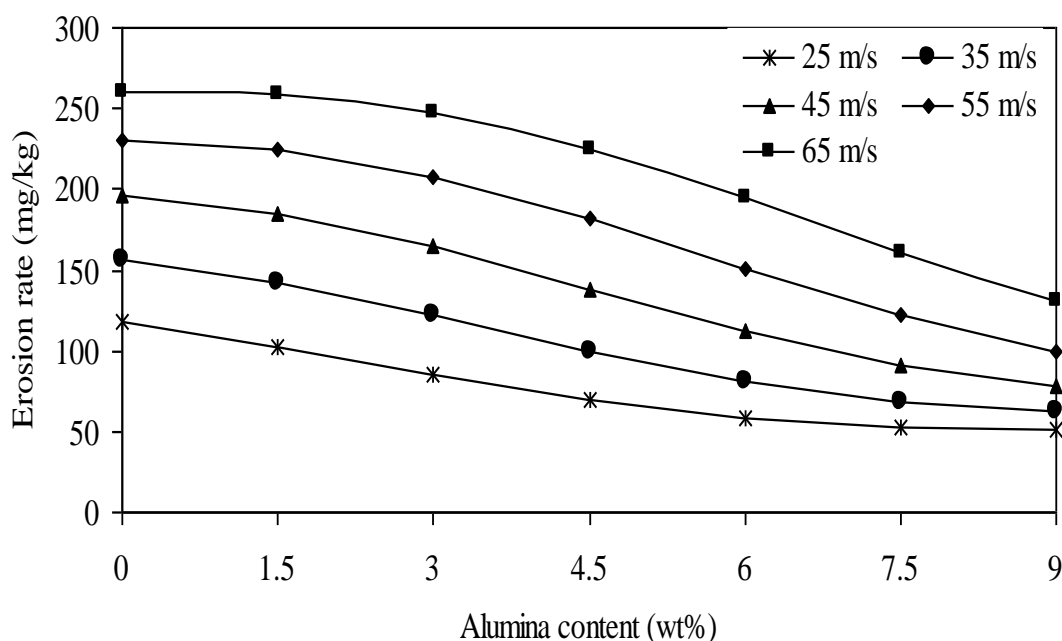


Figure 5.5 Predicted evolution of erosion rate of $\text{Al}_2\text{O}_3/\text{ZA-27}$ metal matrix composites with filler content (at stand-off-distance 55 mm and erodent temperature 140°C)

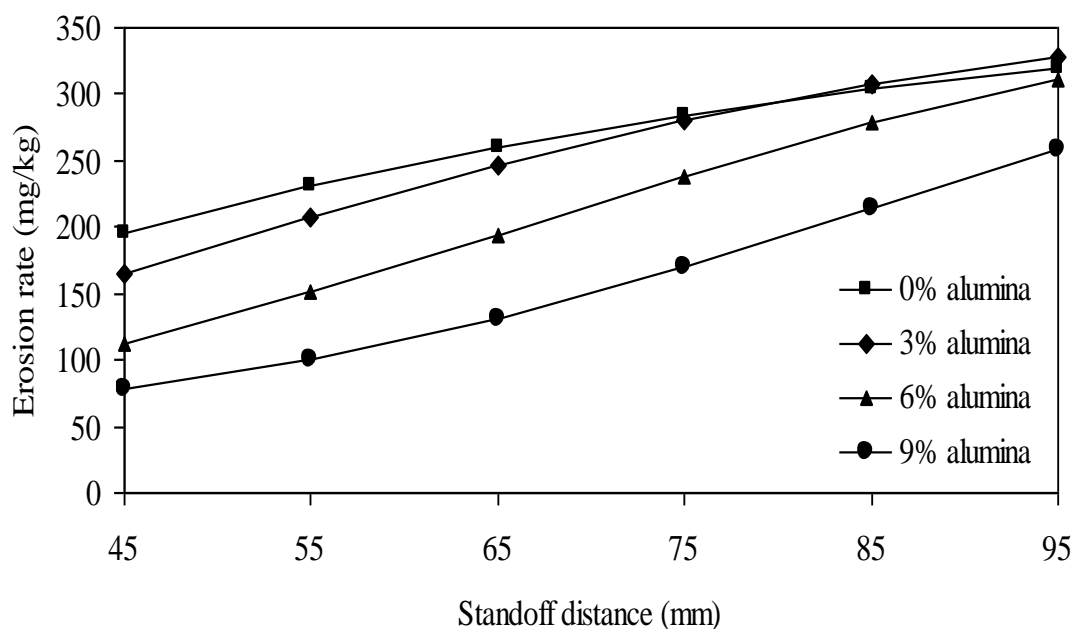


Figure 5.6 Predicted evolution of erosion rate of $\text{Al}_2\text{O}_3/\text{ZA-27}$ metal matrix composites with filler content (at impact velocity 65 m/s and erodent temperature 140°C)

Chapter Summary

This chapter has provided a critical analysis on the solid particle erosion characteristics of alumina particulate filled ZA-27 metal matrix composites using Taguchi experimental design. Significant control factors affecting the wear rate have been identified through successful implementation of this technique. It has been concluded that the impact velocity is the most significant control factor followed by the filler content affecting the erosion wear rates of this particulate filled metal matrix composites. This chapter also includes a morphological study of the eroded surfaces of the composites.

The research presented in this chapter further illustrates that the use of a neural network model to simulate experiments with parametric design strategy is effective, efficient and helps to predict the wear response of particulate filled ZA-27 metal matrix composites under different test conditions within and beyond the experimental domain. The predicted and the experimental values of wear rate exhibit good agreement and validate the remarkable prediction capability of a well-trained neural network for this kind of processes.

The next chapter presents the research findings related to the erosion response of SiC/ZA-27 metal matrix composites.

Chapter 6

Results and Discussion: Part- 3

**Erosion Wear Characteristics of SiC / ZA-27
Metal Matrix Composites**

RESULTS AND DISCUSSION: (PART-3)

Erosion Wear Characteristics of SiC / ZA-27 Metal Matrix Composites

This chapter presents the experimental findings related to the erosion wear characteristics of silicon carbide filled ZA-27 metal matrix composites under different test conditions. Critical parametric analysis of the test results using Taguchi method and simulated wear predictions using artificial neural network model are also presented.

6.1 Surface Morphology

Some typical SEM micrographs of the uneroded and eroded surfaces of SiC filled ZA-27 alloy composites are shown in Figure 6.1. The surface of the composite with 9 wt% of SiC before being subjected to solid particle erosion, shown in Fig.6.1a, appears to be smooth with no wear grooves. Shallow wear tracks are observed on the composite surface (Figure 6.1b) when eroded with at low impact velocity (35 m/sec). With an increase in impact velocity from 35 to 45 m/sec for these particulate filled composite, the worn surface shows formation of grooves along with patches of damaged regions as shown in Figure 6.1c. On further increase in impact velocity (i.e. 65 m/sec), deeper wear grooves, micro-cracks and fragmented dispersed phase are observed as in Figure 6.1d. The extent of deformation thus increases with the increase in impact velocity and breaking of micro-constituents in the regions close to the wear surface. Micro-cracking in the top layer of the subsurface region is also observed and the flow of micro-constituents in the direction of erodent flow in the nearest vicinity of wear surface is another feature observed in the micrograph shown in Figure 6.1d.

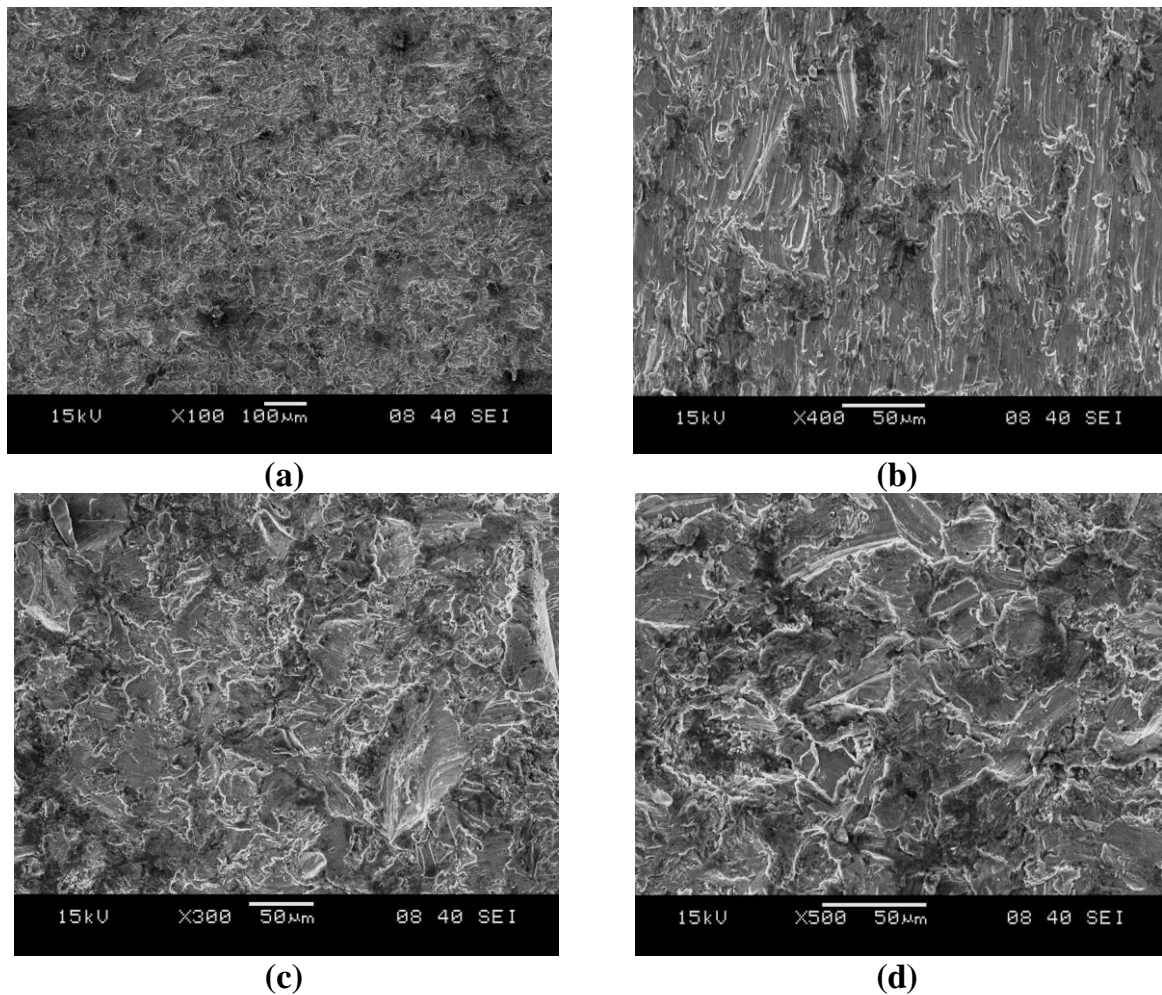


Fig. 6.1 SEM micrographs of the uneroded and eroded surfaces of the ZA27 metal matrix composites filled with 9 wt% SiC

6.2 Erosion Test Results and Taguchi Analysis

The erosion wear rates of SiC reinforced ZA-27 metal matrix composites under various test conditions are given in Table 6.1. The experimental observations are transformed into a signal-to-noise (S/N) ratios. In the Table 6.1, the last column represents S/N ratio of the erosion rate which is in fact the average of three replications. There are several S/N ratios available depending on the type of characteristics. The S/N ratio for minimum erosion rate coming under *smaller-is-better* characteristic can be calculated as logarithmic transformation of the loss function as shown below:

$$S/N = -10 \log \frac{1}{n} \sum y^2 \quad (6.1)$$

where, n the number of observations, and

y the observed data.

The overall mean for the S/N ratio of the erosion rate is found to be – 42.4323 dB. The analysis is made using the popular software specifically used for design of experiment applications known as MINITAB 14.

Test Run	Impact Velocity (A) m/sec	Stand-off distance (B) mm	Erodent temp. (C) °C	Impingement angle (D) degree	Filler content (E) wt %	Erosion rate (Er) mg/kg	Signal to noise ratio (S/N) db
1	35	55	35	45	0	145.667	-43.2672
2	35	65	70	60	3	90.265	-39.1104
3	35	75	105	75	6	63.364	-36.0369
4	35	85	140	90	9	33.540	-30.5113
5	45	55	70	75	9	103.452	-40.2948
6	45	65	35	90	6	120.256	-41.6021
7	45	75	140	45	3	155.965	-43.8605
8	45	85	105	60	0	194.888	-45.7957
9	55	55	105	90	3	185.824	-45.3820
10	55	65	140	75	0	221.333	-46.9009
11	55	75	35	60	9	98.134	-39.8364
12	55	85	70	45	6	120.354	-41.6092
13	65	55	140	60	6	241.230	-47.6486
14	65	65	105	45	9	133.600	-42.5161
15	65	75	70	90	0	243.333	-47.7240
16	65	85	35	75	3	220.601	-46.8721

Table 6.1 Erosion wear test results with the corresponding S/N ratios

Level	A	B	C	D	E
1	-37.23	-44.15	-42.89	-42.81	-45.92
2	-42.89	-42.53	-42.18	-43.10	-43.81
3	-43.43	-41.86	-42.43	-42.53	-41.72
4	-46.19	-41.20	-42.23	-41.30	-38.29
Delta	8.96	2.95	0.71	1.79	7.63
Rank	1	3	5	4	2

Table 6.2 Response table for signal to noise ratios

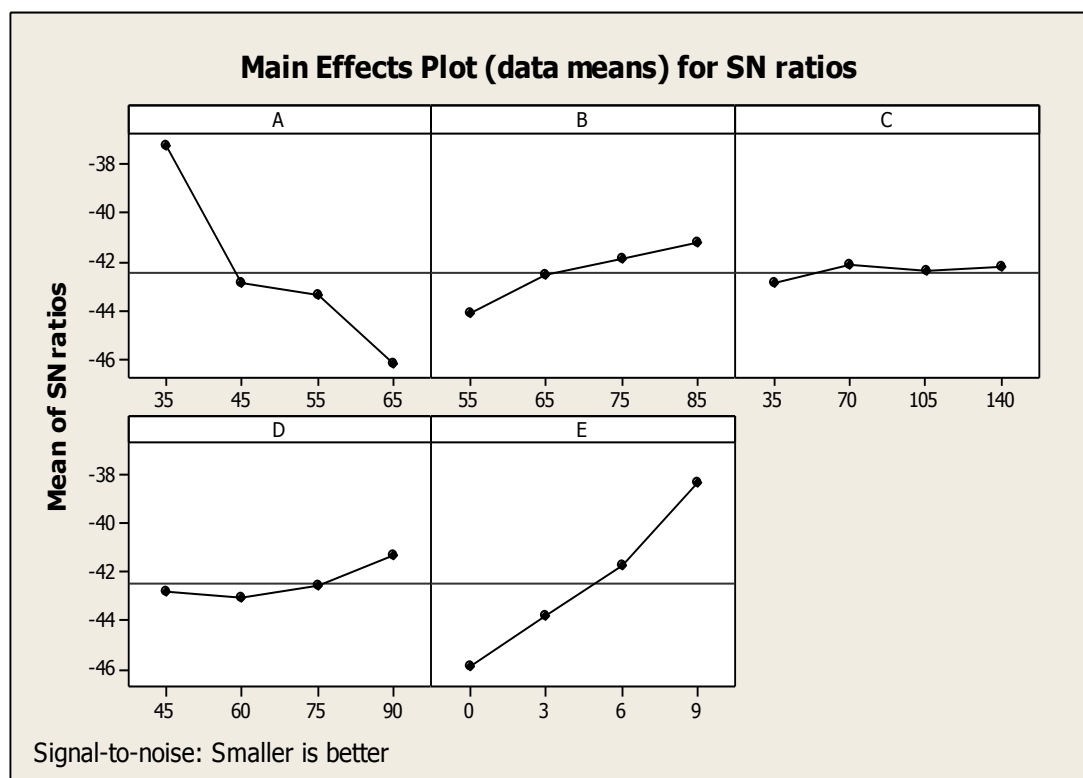


Figure 6.2 Effect of control factors on erosion rate

The S/N ratio response is given in the Table 6.2, from which it can be concluded that among all the factors, impact velocity is the most significant factor followed by filler content, stand-off-distance and impingement angle while the erodent temperature has the least or negligible significance on erosion rate of these SiC filled ZA-27 metal matrix composites. It also leads to the conclusion that factor combination of A1, B4, C2, D4 and E4 gives minimum erosion wear rate.

6.3 Factor Settings for Minimum Erosion Rate

In this study, an attempt is made to derive optimal settings of the control factors for minimization of erosion rate and a predictive equation is developed for determination of erosion rate in terms of the three most influential control factors. The single-objective optimization requires quantitative determination of the relationship between erosion rates with combination of control factors. In order to express, erosion rate in the form of a mathematical model, the following correlation is suggested.

$$\mathbf{E_r}=\mathbf{K_0}+\mathbf{K_1}\times\mathbf{A}+\mathbf{K_2}\times\mathbf{B}+\mathbf{K_3}\times\mathbf{D}+\mathbf{K_4}\times\mathbf{E} \quad (6.5)$$

Here, $\mathbf{E_r}$ is the performance output term i.e. the erosion rate in mg/kg and $\mathbf{K_i}$ ($i = 0, 1, 2, 3, 4$) are the model constants. \mathbf{A} is the impact velocity (m/s), \mathbf{B} is the stand-off-distance (mm), \mathbf{D} is the impingement angle (degree) and \mathbf{E} is the filler content (wt.%). The constants are calculated using non-linear regression analysis with the help of SYSTAT 7 software and the following relations are obtained.

$$\mathbf{E_r} = \mathbf{54.682} + \mathbf{3.922}\times\mathbf{A} - \mathbf{0.813}\times\mathbf{B} + \mathbf{0.111}\times\mathbf{D} - \mathbf{11.808}\times\mathbf{E} \quad (6.6)$$

A comparison between experimental values and values obtained using this predictive equation for erosion rate along with corresponding percentage errors are given in Table 6.3. It is noted that the errors associated with the predictive values in regard to the experimental ones lie between 0- 22% for most of the test

runs. The correctness of the calculated constants is also confirmed as a high correlation coefficient (r^2) in the tune of 0.989 is obtained for Equation 6.5 and therefore, the model is quite suitable to use for further predictive purpose.

Sl. No	Erosion Rate (mg/kg)		
	<i>Results obtain from predictive equation</i>	<i>Results obtain from experiment</i>	<i>Error Percentage</i>
1	152.232	145.667	4.506855
2	110.343	90.265	22.24339
3	68.454	63.364	8.032952
4	26.565	33.54	20.7961
5	88.51	103.452	14.4434
6	117.469	120.256	2.31756
7	139.768	155.965	10.385
8	168.727	194.888	13.4236
9	200.243	185.824	7.759493
10	225.872	221.333	2.050756
11	109.805	98.134	11.89292
12	135.434	120.354	12.5297
13	200.709	241.23	16.7977
14	155.49	133.6	16.38473
15	258.627	243.333	6.285214
16	213.408	220.601	3.26064

Table 6.3 Comparison of the experimental and the predictive erosion rates

6.4 Analysis and Prediction of Erosion Response using ANN

As mentioned earlier, artificial neural network (ANN) is a technique that involves database training to predict input-output evolutions. In this attempt to simulate the erosion wear process and to predict the erosion rate under different operating conditions for SiC/ZA-27 metal matrix composites, different ANN structures are tested and based on least error criterion, one structure, is selected for training of the input-output data which is presented in Table 6.4. The optimized three layer neural network used in this simulation is illustrated in Figure 6.3.

Input parameter for training	Values
Error tolerance	0.003
Learning parameter (β)	0.002
Momentum Parameter (α)	0.002
Noise Factor (NF)	0.001
Number of iteration	10, 000, 000
Slope parameter (ϵ)	0.6
Number of layers	3
Number of neurons in input layer (I)	4
Number of neurons in hidden layer (H)	12
Number of neurons in output layer (O)	1

Table 6.4 Input parameters selected for training

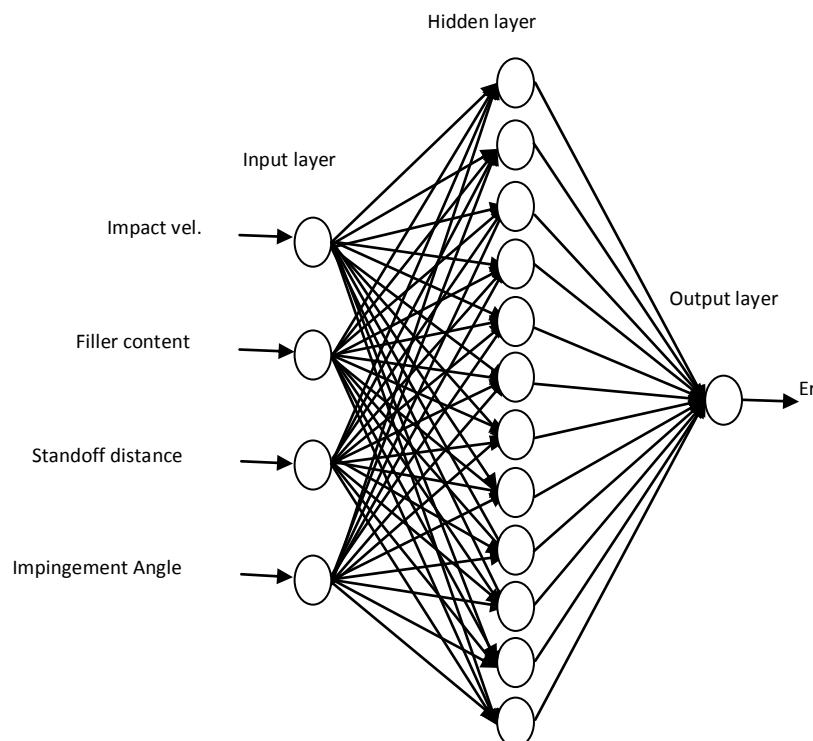


Figure 6.3 The three-layer neural network.

The ANN predictive results of erosion wear rate for all the 16 test conditions are shown and compared with the experimental values along with the associated percentage errors in Table 6.5. It is observed that the errors lie in the range of 0 - 10% which establishes the validity of the neural computation. The errors, however, can still be reduced and the quality of predictions can be further improved by enlarging the datasets and by optimizing the construction of the neural network.

Erosion Rate (mg/kg) Experimental value	Erosion Rate (mg/kg) ANN predicted value	Error Percentage (%)
145.667	148.667	2.059492
90.265	93.266	3.324655
63.364	57.594	9.10612
33.540	35.646	6.27907
103.452	102.015	1.38905
120.256	115.731	3.76281
155.965	145.323	6.82333
194.888	177.705	8.81686
185.824	185.27	0.29813
221.333	222.55	0.54985
98.134	101.852	3.788697
120.354	132.217	9.856756
241.230	238.23	1.24363
133.600	145.712	9.02994
243.333	240.329	1.23452
220.601	224.485	1.760645

Table 6.5 Comparison of the experimental and the ANN predicted erosion rates under similar test conditions

A well-trained ANN is expected to be very helpful for the analysis of erosion wear characteristics of any given composite and permits to study quantitatively the effect of each of the considered input parameters on the wear rate. The range of any chosen parameter can be beyond the actual experimental limits, thus offering the possibility to use the generalization property of ANN in a large parameter space. In the present investigation, this possibility has been explored by selecting the significant factors i.e. the impact velocity and filler content in a range wider than that of the experimental domain. Sets of predictions for erosion rate of SiC/ZA-27 metal matrix composites of different filler content are evolved and these predicted evolutions are illustrated in Figures 6.4, 6.5, 6.6 and 6.7.

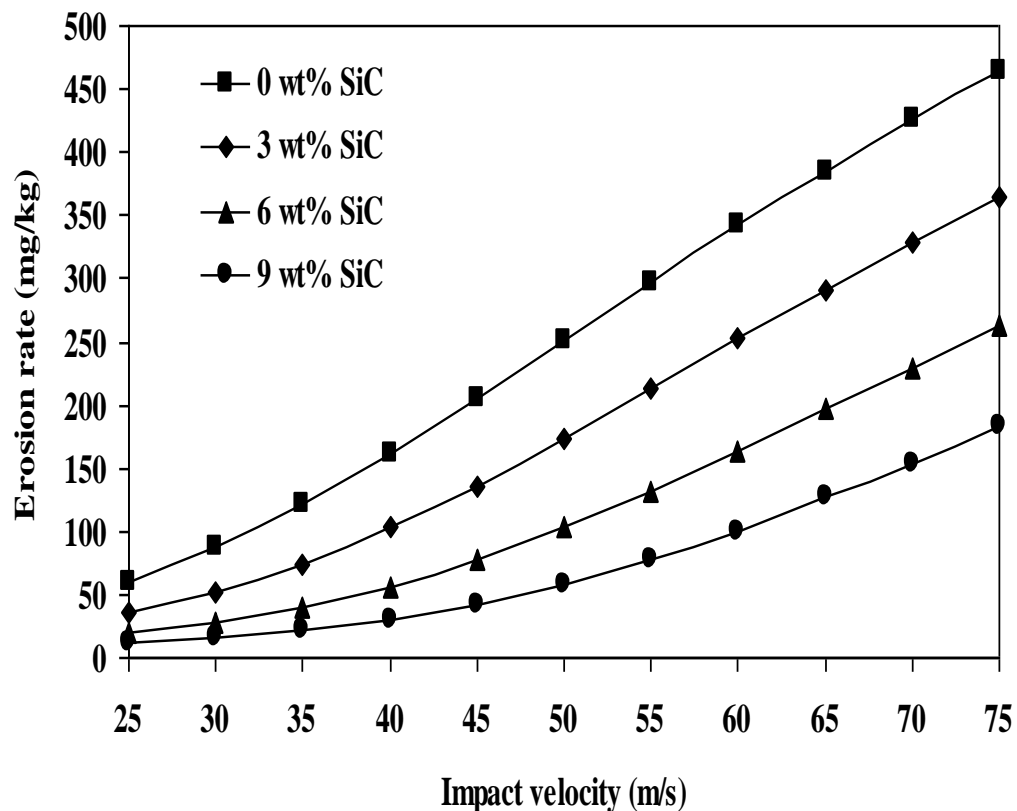


Figure 6.4 Predicted evolution of erosion rate of SiC/ZA-27 metal matrix composites with impact velocity (at stand-off-distance 85 mm and impingement angle 45°)

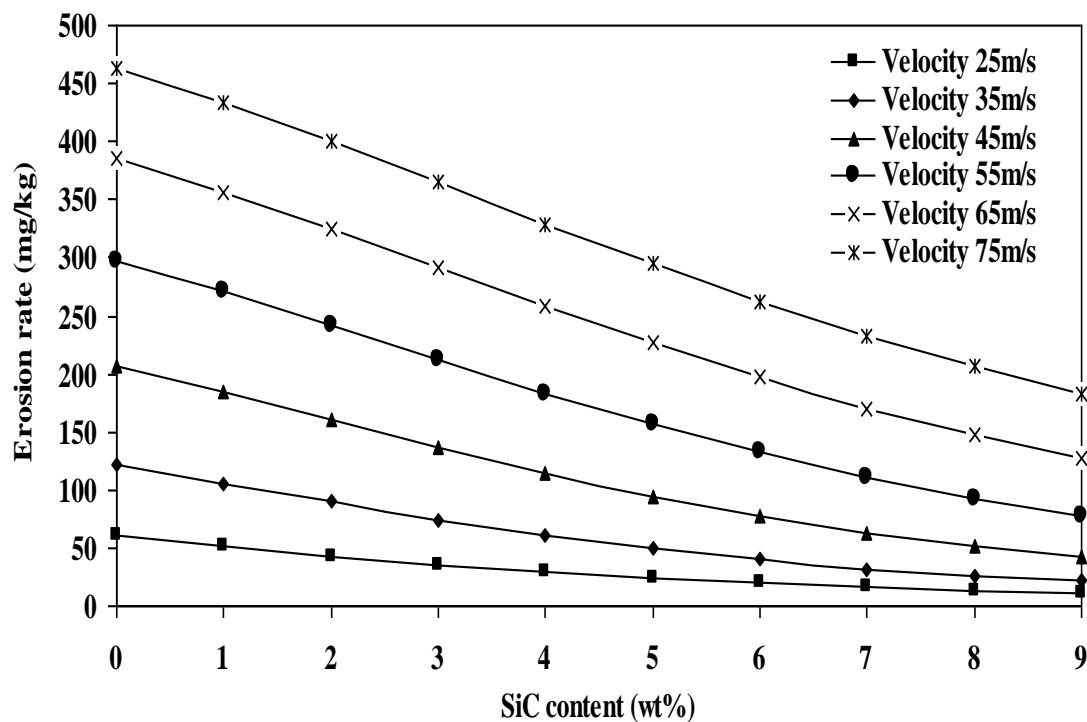


Figure 6.5 Predicted evolution of erosion rate of SiC/ZA-27 metal matrix composites with filler content (at stand-off-distance 85 mm and impingement angle 45°)

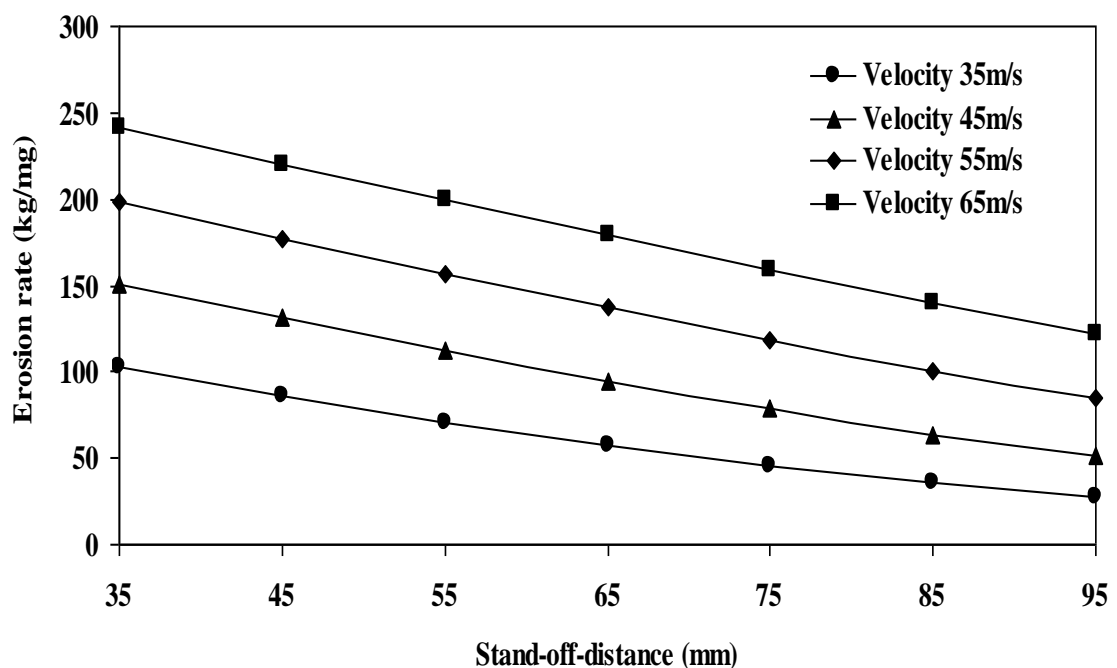


Figure 6.6 Predicted evolution of erosion rate of SiC/ZA-27 metal matrix composites with stand-off-distance (at filler content 9 wt% and impingement angle 90°)

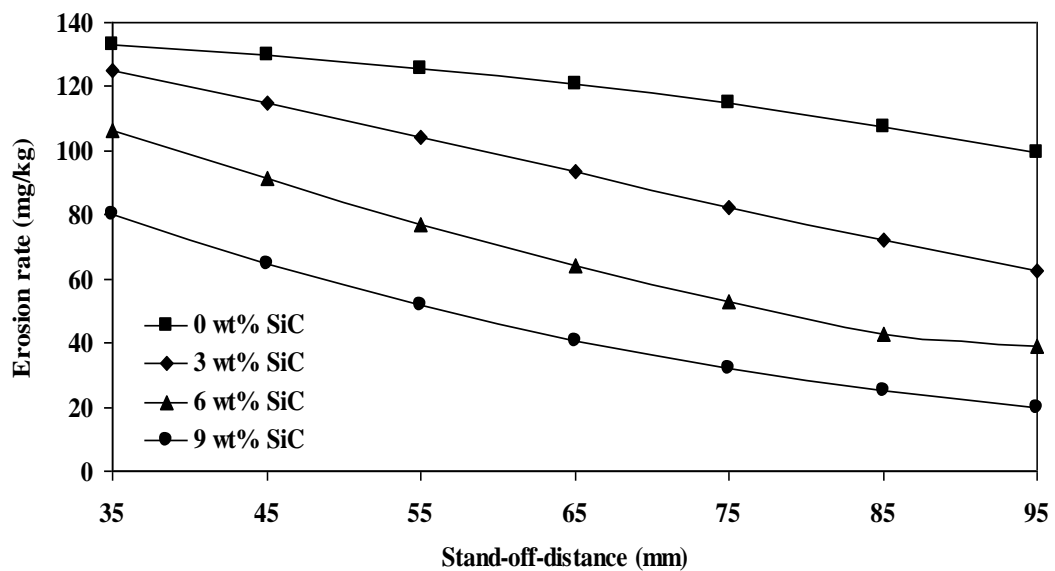


Figure 6.7 Predicted evolution of erosion rate of SiC/ZA-27 metal matrix composites with stand-off-distance (at impact velocity 35m/s and impingement angle 60°)

6.5 Comparison of Al_2O_3 and SiC reinforced ZA-27 MMCs

Figure 6.8 shows the comparison of erosion wear rates of ZA-27/ Al_2O_3 and ZA-27/SiC MMCs eroded under similar test conditions. It is evident from the comparison graph that the erosion rate of ZA-27/ Al_2O_3 composites at any particular test condition is higher than that of ZA-27/SiC composites under the same test condition.

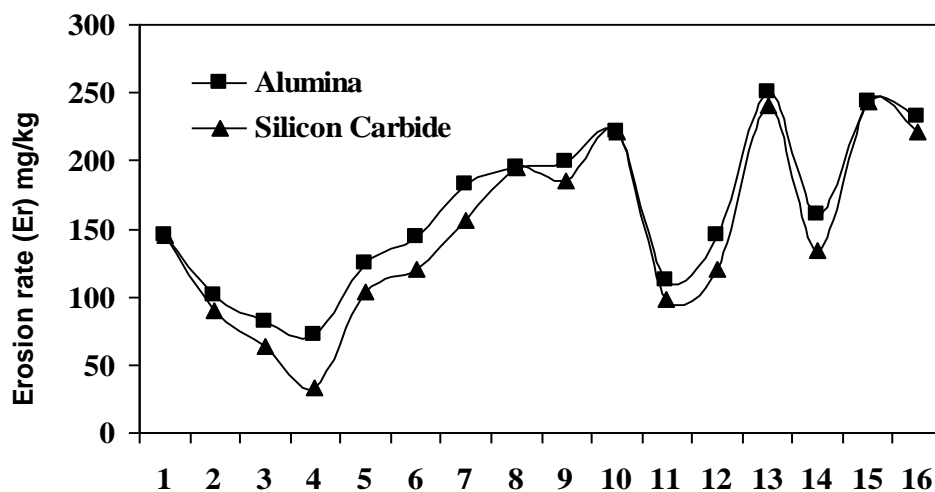


Figure 6.8 Comparisons between the erosion response of ZA-27/ Al_2O_3 and ZA-27/SiC MMCs under similar test conditions

Silicon carbide is known to be harder than alumina and subsequently the composites with SiC are found to exhibit higher hardness than the composites filled with Al_2O_3 . The improvement of bulk hardness contributes to the enhancement of resistance to wear. Thus the better erosion resistance of ZA-27/SiC composites is attributed to the higher bulk hardness. SiC particles, being hard dispersoids, act as barriers for the movement of dislocations within the composite and hence increase the hardness. Further, the increase in filler content reduces the inter particle distance between these hard particles causing increase in the dislocation pile up and there is a restriction to the plastic flow due to the dispersion of these particles.

Chapter Summary

This chapter has provided a critical analysis on the erosion characteristics of SiC filled ZA-27 metal matrix composites using Taguchi experimental design. Significant control factors affecting the wear rate have been identified through successful implementation of this technique. This chapter also includes a morphological study of the eroded surface of the composites. The research presented in this chapter further illustrates that the use of a neural network model to simulate experiments with parametric design strategy is effective, efficient and helps to predict the wear response of particulate filled ZA-27 metal matrix composites under different test conditions within and beyond the experimental domain. The predicted and the experimental values of wear rate exhibit good agreement and validate the remarkable prediction capability of a well-trained neural network for this kind of processes.

The next chapter provides the summary of the research findings and outlines specific conclusions drawn from this work. Ideas and directions for future research are also suggested.

Chapter 7

Summary and Conclusions

Summary and Conclusions

The research reported in this thesis broadly consists of two parts:

- The first part has provided the description of the materials used and the fabrication details of particulate filled ZA-27 metal matrix composites. The experimental details related to their physical and mechanical characterization are also reported.
- The second part has reported the effect of two different particulate fillers i.e. alumina and silicon carbide on the solid particle erosion characteristics of the ZA-27 metal matrix composites through experimental trials. Parametric appraisal of the erosion process along with wear rate assessment using prediction tools has also been reported in this part of the thesis.

7.1 Summary of the Research Findings

The present work has reported the performance of a new class of metal matrix composites with emphasis on the general trends observed in their properties and behaviour. With the incorporation of particulate fillers, the tensile and flexural strengths of the composites are found to be decreasing in most of the cases. This decline in strength may be attributed to two reasons: one possibility is that the due to the presence of pores at the interface between the filler particles and the matrix, the interfacial adhesion may be too weak to transfer the stress. Hardness and impact strength values have been found to have improved invariably for all the composites on addition of particulate fillers, irrespective of the type of filler. This may be due to the matrix phase and the solid filler phase would be pressed together and touch each other more tightly during hardness and impact tests. Thus, the interface can transfer pressure more effectively although the interfacial bond may be poor. The erosion wear rates of particulate filled ZA-27 MMCs are

found to be lower than those of the unfilled composites under similar test conditions. This has led to the conclusion that the presence of particulate fillers improves the erosion wear resistance of particulates reinforced metal matrix composites. The reduction in material loss in these particulate filled composites can be attributed to two reasons. One is the improvement in the bulk hardness of the composite with addition of these hard filler particles. Secondly, during the erosion process, the filler particles absorb a good part of the kinetic and thermal energy associated with the erodent.

7.2 Conclusions

This analytical and experimental investigation on particulate filled ZA-27 MMCs has led to the following specific conclusions:

1. Successful fabrication of ZA-27 metal matrix composites with reinforcement of conventional ceramic fillers such as Al_2O_3 and SiC is possible using stir casting method.
2. These composites possess very low amount of porosity and improved micro-hardness and impact strength. However, they exhibit slightly inferior tensile and flexural strengths than those of the pure ZA-27 alloy.
3. Erosion characteristics of these composites can also be successfully analyzed using Taguchi experimental design scheme. Taguchi method provides a simple, systematic and efficient methodology for the optimization of the control factors. Significant factors affecting the erosion rate of composites are identified through successful implementation of signal-to-noise response approach. Among the all factors, impact velocity and filler content are found to be most significance factors on the erosion rate of ZA-27 metal matrix composites filled with both fillers.
4. Predictive model based on artificial neural networks (ANN) approach is successfully applied in this investigation to predict and simulate the wear response of the composites under various test conditions within and beyond the experimental domain. The predictions of wear rates as functions of filler

content and testing conditions thus prove a remarkable capability of well-trained neural networks for modeling concern.

7.3 Recommendations for potential applications

The particulate filled ZA-27 metal matrix composites fabricated and experimented upon in this investigation are found to have adequate potential for a wide variety of applications particularly in erosive environment. In aerospace industries it can be used in structural landing gear component F16 aircraft, blade sleeves for the eurocopter, jet engine–fan exit guide vanes etc. Applications in surface transport are brake rotors for high speed train and automotives, automotive engine cylinder liner, automotive engine exhaust valves and connecting rods. In sports as mountain bikes, in power generation sector this material can be used in light-weight composite core for power lines. Also most widely it is used in bearing.

7.4 Scope for future work

This work leaves a wide scope for future investigators to explore many other aspects of such particulate filled ZA-27 metal matrix composites. Some recommendations for future research include:

- Study on the response of these composites to other wear modes such as abrasion, dry sliding and slurry erosion.
- Exploration of new fillers like metal nitrides and industrial wastes etc. for development of such composite materials.

REFERENCES

References

1. Mathews, F.L. and Rawlings, R.D., (1994). Composite Materials; Engineering and Science, Chapman and Hall,.
2. Park, B. G., (2001). Material characterisation and mechanical properties of Al₂O₃-Al metal matrix composites, *Journal of Materials Science* 36, 2417 – 2426
3. Stolarski T. A, (1990). Tribology in Machine Design, Heiman Newnes, UK.
4. Päivi Kivikytö-Reponen, (2006). Correlation of Material Characteristics and Wear of Powder Metallurgical Metal Matrix Composites, Doctoral Theses in Materials and Earth Sciences, Helsinki University of Technology, Laboratory of Materials Science, Espoo.
5. Budinski K. G, (1998). Surface Engineering for Wear Resistance, Prentice Hall, New Jersey.
6. Robinowicz E, (1965). Friction and wear of materials, John Willey, New York, USA.
7. Kosel T. H., (1992). Solid Particle Erosion, ASM Handbook, ASM International, 18, 199-213. (T.H. Kosel. In: P.J. Blau, Editor, Friction, Lubrication and Wear Technology, ASM Handbook, 18, pp. 207).
8. Mei, Z., Zhu, Y.H., Lee, W.B., Yue, T.M. and Pang, G.K.H., (2006). Composites: Part A 37, 1345–1350
9. Ranganath, G., Sharma, S.C. and Krishna, M., (2001). Dry sliding wear of garnet reinforced zinc/aluminium metal matrix composites, *Wear* 251, 1408–1413
10. Kumar, M. P., Sadashivappa, K., Prabhukumar, G. P. and Basavarajappa, S., (2006). Dry Sliding Wear Behaviour of Garnet Particles Reinforced Zinc-Aluminium Alloy Metal Matrix Composites, ISSN 1392–1320, materials science, Vol. 12, No. 3.
11. Rohatgi, P. K., (1993). Metal-matrix Composites, *Defence Science Journal*, Vol 43, No 4, 323-349.
12. Bandyopadhyay, N. R., Ghosh, S. and Basumallick, A., (2007). New Generation Metal Matrix Composites, *Materials and Manufacturing Processes*, 22: 679–682.
13. Chou, T.W., Kelly, A. and Okura, A., (1985). Fibre-reinforce metal-matrix composites, *COMPOSITES. VOLUME 16. NO 3*, 187-206
14. Avila, A. F. and Tamma, K. K.(1998) 'Analysis of Laminate Metal Matrix Composites', *Journal of Thermal Stresses*, 21: 9, 897 — 917

15. Pramanik, A., Zhang, L.C. , Arsecularatne, J.A., (2007). An FEM investigation into the behavior of metal matrix composites: Tool–particle interaction during orthogonal cutting, *International Journal of Machine Tools & Manufacture*, 47, 1497–1506
16. Shoukry, S. N. , Prucz, J. C. , Shankaranarayana, P. G. and William, G. W.(2007) 'Microstructure Modeling of Particulate Reinforced Metal Matrix Composites', *Mechanics of Advanced Materials and Structures*, 14: 6, 499 — 510.
17. Jayamathy, M. , Seshan, S. , Kailas, S. V. , Kumar, K. and Srivatsan, T. S.(2005) 'Influence of Reinforcement And Processing on The Wear Response of Two Magnesium Alloys', *Materials and Manufacturing Processes*, 20: 2, 255 — 271
18. Melgarejo, Z. H., Suárez, O. M. and Kumar S., (2008). Microstructure and properties of functionally graded Al–Mg–B composites fabricated by centrifugal casting, *Composites: Part A* 39, 1150–1158.
19. Delannay E., Colin, C., Marchal, Y., Tao, L., Boland, F., Cobzaru, P., Lips, B. and Dellis, M. A., (1993). Processing and properties of metal matrix composites reinforced with continuous fibers for the control of thermal expansion, creep resistance and fracture toughness, *Journal De Physique IV*, Volume 3, 1675-1684
20. Veeresh Kumar, G. B., Rao, C. S. P., Selvaraj, N., Bhagyashekar, M. S., (2010). Studies on Al6061-SiC and Al7075-Al₂O₃ Metal Matrix Composites, *Journal of Minerals & Materials Characterization & Engineering*, Vol. 9, No.1, 43-55.
21. Kennedy, A. R, (2002). The microstructure and mechanical properties of Al-Si-B₄C metal matrix composites, *Journal of Materials Science* 37, 317– 323.
22. Takei, T, Hatta, H and Taya, M, (1991). Thermal Expansion Behavior of Particulate-filled Composites in Single Reinforcing Phase, *Materials Science and Engineering*, A131, 133-143.
23. Ranganath, S, (1997). A Review on Particulate-reinforced titanium matrix composites, *Journal of Materials Science*, 32(1), 1-16.
24. Ala-Klemea, S., Kivikytö-Reponenb, P., Liimatainenb, J., Hellmanb, J. and Hannulaa, Simo-Pekka, (2006). Abrasive wear properties of metal matrix composites produced by hot isostatic pressing, *Proc. Estonian Acad. Sci. Eng.*, 12, 4, 445–454

25. Basavarajappa, S., Chandramohan, G. and Davim, J. P., (2007). Application of Taguchi techniques to study dry sliding wear behaviour of metal matrix composites, *Materials and Design* 28, 1393–1398
26. Shipway, P.H., Kennedy, A.R. and Wilkes, A.J., (1998). Sliding wear behaviour of aluminium-based metal matrix composites produced by a novel liquid route, *Wear* 216, 160-171
27. Chen, R., Akira Iwabuchi b. Tomoharu Shimizu tL Hyung Seop Shin ~, Hidenobu Mifune The sliding wear resistance behavior of NiAl and SiC particles reinforced aluminum alloy matrix composites, *Wear* 213 (tt)t.~7) 175-184
28. Melgarejo, Z. H., Sua´rezb, O. M., and Kumar S., (2006). Wear resistance of a functionally-graded aluminum matrix composite, *Scripta Materialia*, 55, 95–98
29. Kumar, S., Sarma, V. S., Murty, B.S., (2008). A statistical analysis on erosion wear behaviour of A356 alloy reinforced with in situ formed TiB₂ particles, *Materials Science and Engineering A*, 476, 333–340.
30. Alman, D.E., Tylczak, J.H., Hawk, J.A., Hebsur, M.G., (1999). Solid particle erosion behavior of an Si₃N₄–MoSi₂ composite at room and elevated temperatures, *Materials Science and Engineering A*, 261, 245–251.
31. Moutsatsou, A., Itskos, G. S., Koukouzas, N. and Vounatsos, P., (2009). Synthesis of aluminum-based metal matrix composites (MMCs) with lignite fly ash as reinforcement material, 2009 world of coal ash (WOCA0 conference).
32. Rajan, T.P.D., Pillai, R.M., Pai, B.C., Satyanarayana, K.G., Rohatgi, P.K., (2007). Fabrication and characterisation of Al–7Si–0.35Mg/fly ash metal matrix composites processed by different stir casting routes, *Composites Science and Technology*, 67, 3369–3377.
33. Acharya, S. K., Dikshit, V. And Mishra, P., (2008). Erosive Wear Behaviour of Redmud Filled Metal Matrix Composite, *Journal of REINFORCED PLASTICS AND COMPOSITES*, Vol. 27, No. 2.
34. Modi, O.P., Prasad, B.K., Jha, A.K., (2006). Influence of alumina dispersoid and test parameters on erosive wear behaviour of a cast zinc–aluminium alloy, *Wear*, 260, 895–902.
35. Li, B.J. and Chao, C.G., (1996). *Metallurgical Matl. Trans.* 27, 809-818.

36. Tjong, S.C. and Chen, F., (1997). Wear Behavior of As-Cast ZnAl27/SiC Particulate Metal-Matrix Composites under Lubricated Sliding Condition. *Metallurgical and Materials Transactions A*; 28a:1951-5.
37. Tjong, S. C. , (2007). Novel Nanoparticle-Reinforced Metal Matrix Composites with Enhanced Mechanical Properties, *Advanced Engineering Materials*, 9, No. 8
38. Doe, T. J. A. and Bowen, P., (1996). Tensile properties of particulate-reinforced metal matrix composites, *Composites Part A*, 27A, 655-665.
39. Pardo, A., Merino, M. C., Merino, S., Lopez, M. D., Viejo, F. and Carboneras, M., (2003). Influence of reinforcement grade and matrix composition on corrosion resistance of cast aluminium matrix composites (A3xx.x/SiCp) in a humid environment, *Materials and Corrosion* 54, 311–317.
40. Chen, Q., Li, D.Y., (2003). Computer simulation of solid-particle erosion of composite materials, *Wear*, 255, 78–84.
41. Pukanszky, B., and Voros, G., (1993). Mechanism of interfacial interactions in particulate filled composite, *Composite Interfaces*, 1(5), 411-427.
42. Ilegbusi, O. J. and Yang, J., Porosity Nucleation in Metal-Matrix Composites, *Metallurgical And Materials Transactions A Volume 31A*, 2000—2069.
43. Surappa, M. K., (2003). Aluminium matrix composites: Challenges and opportunities, *Sadhana Vol. 28, Parts 1 & 2*, 319–334.
44. Chawla, N., (2001). Mechanical behaviour of particle reinforced metal matrix composites, *Advanced engineering materials*.
45. Sharma, S.C., Girish, B.M., (1999). Fractography, Fluidity and Tensile properties of aluminium hematite particulate composites, *JMEPEG* 8:309-314.
46. Stone, R.H.V., Cox, T. B., Low, J.R., (1985). *Int.Mater.Rev*, Vol30, 157
47. Poddar, P., (2009). The microstructure and mechanical properties of SiC reinforced magnesium based rheocasting process, *JMEPEG*, 849-855.
48. Sharma, S.C., (1999). Mechanical properties and fractography of zircon particle reinforced ZA-27alloy composite materials, *composite science and technology*, 1805-1812.
49. Sharma, S.C., (1997). Mechanical .properties and fractography of cast lead / quartz particulate composites, *materials and design*, vol-18, 149-153.

50. Kok, M., (2005). Production and mechanical properties of Al₂O₃ particle reinforced 2024 aluminium alloy composites, *Journal of materials processing technology*, 381-387.
51. Abdizadeh, H., (2011). Improvement in physical and mechanical properties of aluminium /zircon composites fabricated by powder metallurgy method, *materials and design*, 4417-4423.
52. Kataiah, G. S., (2010). The mechanical properties and fractography of aluminium 6061-TiO₂ composites, *International journal of pharmaceutical studies and research*, vol-1, 17-25.
53. Mares, M., (2001). Some issues on tailoring possibilities for mechanical properties of particulate reinforced metal matrix composites, *Journal of optoelectronics and advanced materials*, vol-3, 119-124.
54. Seah, K. H. W., Sharma, S. C. and Girish, B. M., (1997). Mechanical properties of as-cast and heat-treated ZA-27/graphite particulate composites, *Composites Part A*, 28A, 251-256.
55. Li, Y., Ngai, T. L., Xia, W., Zhang, Wen., Effects of Mn content on the tribological behaviors of Zn-27% Al-2% Cu alloy, *Weu 198 0996*) 129-135
56. Prasad, B.K., Patwardhan, A.K., and Yegneswaran, A.H., (1998). Microstructure and Property Characterization of a Modified Zinc-Base Alloy and Comparison with Bearing Alloys, *JMEPEG* 7:130-135.
57. Cuvalc, H., Bas, H., (2004). Investigation of the tribological properties of silicon containing zinc–aluminum based journal bearings, *Tribology International*, 37, 433–440.
58. Badisch, E., Ilo, S., Polak, R., (2009). Multivariable Modeling of Impact-Abrasion Wear Rates in Metal Matrix-Carbide Composite Materials, *Tribol Lett* 36:55–62.
59. Seenappa & Sharma, K.V., (2011). Characterization of Mechanical and Micro structural properties of ZA alloys, *International Journal of Engineering Science and Technology (IJEST)*, Vol. 3 No. 3.
60. Modi, O. P., Rathod, S., Prasad, B. K., Jha, A. K., and Dixit, G., (2007). The influence of alumina article dispersion and test parameters on dry sliding wear behavior of Zinc-based alloy, *Tribology International*, 40, 1137-1146.

61. Dominguez, C., Lopez, M. V. M., Ri'os-jara, D., (2002). The influence of manganese on the microstructure and the strength of a ZA-27 alloy, *Journal of Materials Science*, 37, 5123 – 5127.
62. Chen, T., Yuan, C., Fu, M., Ma, Y., Li, Y. and Hao, Y., (2009). Friction and wear properties of casting in-situ silicon particle reinforced ZA27 composites, *China Foundry*, Vol.6 No.1, 1-8.
63. Chen, T. J., Yuan, C. R., Fu, M. F., Ma, Y., Li, Y. D., Hao, Y., (2008). In-situ silicon particle reinforced ZA27 composites. Part I: microstructures and tensile properties. *Materials Science Technology*, 24: 1321-1332.
64. Bobic, I., Jovanovic, M.T., Ilic, N., (2003). Microstructure and Strength of ZA-27-based composites reinforced with Al₂O₃ particle, *Materials Letters*, 57, 1683-88
65. Ranganath, G., Sharma, S.C., Krishna, M., and Muruli, M.S., (2002). A Study of Mechanical Properties and Fractography of ZA-27/Titanium-Dioxide Metal Matrix Composites. *Journal of Materials Engineering and Performance*;11(4): 408-13.
66. Sharma, S. C., Girish, B. M., Somashekar, D. R., Kamath, R., Satish, B. M., (1999). Mechanical Properties and fractography of Zircon-particle-reinforced ZA-27 alloy composite materials, *Composites science and technology*, 59, 1805-1812
67. Babic, M., Slobodan, M., Dzunic, D., Jeremic, B., and Ilija, B., (2010) Tribological Behavior of Composites Based on ZA-27 Alloy Reinforced with Graphite Particles. *Tribology Letters*; 37:401–10.
68. Sharma, S. C., Seah, K. H. W., Satish, B. M., Girish, B. M., (1996). Effect of short glass fibers on the mechanical properties of cast ZA-27 alloy composites, *Materials & Design*, Vol. 17, No. S/6, 245-250.
69. Sharma, S.C., Girish, B.M., Satish, B.M., and Kamath, R., (1998). Aging Characteristics of Short Glass Fiber Reinforced ZA-27 Alloy Composite Materials, *JMEPEG* 7:747-750.
70. Sharma, S.C., (2001). Elastic Properties of Short Glass Fiber-Reinforced ZA-27 Alloy Metal Matrix Composites, *JMEPEG* 10:468–474.

71. Sharma, S.C., Girish, B.M., Kamath, R., Satish, B.M., (1997). Effect of SiC particle reinforcement on the unlubricated sliding wear behaviour of ZA-27 alloy composites, *Wear*, 213, 33-40.
72. Babic, M., Slobodan, M., Fatima, Zivic, Ilija, B., (2010). Wear Behavior of Composites Based on ZA-27 Alloy Reinforced by Al₂O₃ Particles Under Dry Sliding Condition, *Tribol Lett* 38: 337–346.
73. Sharma, S.C. , Girish, B. M., Kramath, R., Satish, B. M., (1998). Graphite particles reinforced ZA-27 alloy composite materials for journal bearing applications, *Wear*, 219, 162-168.
74. Seah, K. H. W., Sharma, S. C. and Girish, B. M., (1995). Mechanical properties of cast ZA27-graphite particulate composites, *Materials and Design*, volume 16 number 5, 271-275.
75. Patnaik, A., Mamatha, T.G., Biswas, S. and Kumar, P., (2011). Damage Assessment of Titania Filled Zinc-Aluminium Alloy Metal Matrix Composites in Erosive Environment: A Comparative Study. *Materials and Design*; 36: 511-21.
76. Biswas, S., (2010). Processing, Characterization and wear response of Particulate Filled Epoxy Based Hybrid Composites, Ph.D. Thesis, NIT, Rourkela, India.
77. Organization for Economic Co-operation and Development, (1969), Research Group on Wear of Engineering Materials, Glossary of terms and definitions in the field of friction, wear and lubrication, *Tribology*, Paris, 169.
78. Barkoula, N. M. and Karger-Kocsis, J., (2002). Review Processes and influencing parameters of the solid particle erosion of polymers and their composites, *Journal of Material Science*, 37 (18), 3807-3820.
79. Burwell, J. T. and Strang, C. D., (1952). On the empirical law of adhesive wear, *Journal of Applied Physics*, 23 (1), 18-28.
80. Burwell (Jr.), J. T, (1957/1958). Survey of Possible Wear Mechanisms, American-Standard Corporation, New York, U.S.A., *Wear*, 1, 19-141.
81. Aquaro, D. and Fontani, E., (2001). Erosion of Ductile and Brittle Materials, *Meccanica* 36: 651–661.
82. Lindsley, B.A. and Marder, A.R., (1998). Solid Particle Erosion of an Fe-Fe₃C Metal Matrix Composite, *Metallurgical and materials Transactions*, Volume 29 A, 1071

83. Das, S., Mondal, D.P., and Sawla, S., (2004). Solid Particle Erosion of Al Alloy and Al-Alloy Composites: Effect of Heat Treatment and Angle of Impingement, *Metallurgical and materials Transactions*, Volume 35 A , 1369
84. Fangu, Q., Sidky, P., Hocking, M. G., (1997). Erosive wear behaviour of aluminium based Composites, *Materials & Design*, Vol. 18, Nos. 4r6, pp. 389-93,
85. Zhou, R., Jiang, Y., Lu, D., (2003). The effect of volume fraction of WC particles on erosion resistance of WC reinforced iron matrix surface composites, *Wear*, 255, 134–138.
86. Flores, J.F., Neville, A., Kapur, N., Gnanavelu, A., (2009). An experimental study of the erosion–corrosion behavior of plasma transferred arc MMCs, *Wear*, 267, 213–222.
87. Kondoha, K., Umedaa, J., Watanabe, R., (2009). Cavitation erosion of aluminum matrix sintered composite with AlN dispersoids, *Wear*, 267, 1511–1515.
88. Das, S., Mondal, D.P., Dasgupta, R., Prasad, B.K., (1999). Mechanisms of material removal during erosion–corrosion of an Al–SiC particle composite, *Wear*, 236, 295–302.
89. Bitter, J. G. A, (1963). A study of erosion phenomena-Part I, *Wear*, 6, 5–21.
90. Bitter, J. G. A, (1963). A study of erosion phenomena-Part II, *Wear*, 6, 169–190.
91. Lehrke, W. D. and Nonnen, F. A., (1975). 1st International Conference on Protection of Pipes, In: (2nd edition), BHRA, Durham, UK, paper G2.
92. Forse, C. and Ball, A., (1983). Proceedings of 6th International Conference on Erosion by Liquid and Solid Impact, In: J.E. Field and N.S. Corney, Editors, Cavendish Laboratory, Cambridge University, Cambridge, UK.
93. Neilson, J. H. and Gilchrist, A., (1968). An Experimental Investigation into Aspects of Erosion in Rocket Motor Tail Nozzles, *Wear*, 11(2), 123-143.
94. Wright, I. G., (1987). High Temperature Erosion in Coal Combustion and Conversion Processes: A Review, *Material Science and Engineering*, 88, 261- 71.
95. Thimot, G., (1979). In: (2nd edition), American Society for Mechanical engineers Youth Forum on Practical Erosion Problems in Fluid Systems and Machinery, Niagara Falls, New York.
96. Carson, S. E. and Runnels, O. D., (1978). In: (2nd edition), Department of Energy Report Co-0003-28, U.S. Department of Energy.

97. Rademarkers, P. L. F., Bos, L., Van Wortel, J. C and Kotster, B. H, (1984). In: Proceedings of Conference on Fluidized Combustion, Institute of Energy, London.
98. Stringer, J. and Drenier, S., (1981). Proceedings of American Power Conference, In: (2nd edition), 43, 943.
99. Sage, W. and Tilly, G. P., (1969). The Significance of Particle Size in Sand Erosion of Small Gas Turbines, Journal of Aeronautical Society, 73, 427–428.
100. Sundararajan, G. and Roy, M., (1997). Solid particle erosion behaviour of metallic materials at room and elevated temperatures, Tribology International, 30 (5), 339-359.
101. Fernandez, J. E., Fernandez, M., MaDel.Rocio, Diaz, R.V. and Navarro, R. T., (2003). Abrasive wear analysis using factorial experiment design, Wear, 255(1–6), 38–43.
102. Spuzic, S., Zec, M., Abhary, K., Ghomashchi, R. and Reid, I., (1997). Fractional design of experiments applied to a wear simulation, Wear, 212(1), 131–139.
103. Prasad, B.K, (2002). Abrasive wear characteristics of a zinc-based alloy and zincalloy/SiC composite, Wear, 252(3–4), 250–263.
104. Deuis, R.L., (1998). Three-body abrasive wear of composite coatings in dry and wet environments, Wear, 214, 112–130.
105. Banerjee, A., Prasad, S.V, Surappa, M.K and Rohatgi, P.K, (1982). Abrasive wear of cast aluminum alloy/zircon particle composites, Wear, 82, 141-151.
106. Mondal, D.P, Das, S., Jha, A.K. and Yegneshwaran, A.H., (1998). Abrasive wear of Al alloy-Al₂O₃ particle composite: a study on the combined effect of load and size of abrasive, Wear, 223, 131–138.
107. Taguchi, G and Konishi, S, (1987). Taguchi Methods: Orthogonal Arrays and Linear Graphs; Tools for Quality Engineering, American Supplier Institute Inc, Dearborn, MI.
108. Taguchi, G., (1990). Introduction to Quality Engineering, Asian Productivity Organization, Tokyo.
109. Phadke, M.S., (1989). Quality Engineering using Robust Design, Prentice-Hall, Englewood Cliffs, NJ.
110. Wu, Y. and Moore, W.H, (1986). Quality Engineering: Product & Process Design Optimization, American Supplier Institute Inc, Dearborn, MI.

111. Logothetis, N. and Haigh, A., (1988). Characterizing and optimizing multiresponse processes by the Taguchi method, *Qual. Reliab. Eng. Int.*, 4(2), 159–169.
112. Shoemaker, A.C and Kackar, R.N, (1988). A methodology for planning experiments in robust product and process, *Qual. Reliab. Eng. Int.*, 4, 95–103.
113. Sarle, W. S, (1997). Neural network FAQ: Part 1 of 7—Introduction, periodic posting to the Usenet newsgroup comp.ai.neural-nets. Available from: <ftp://ftp.sas.com/pub/neural/FAQ.html>
114. Maier, H. R., Dandy, G. C., *Environmental Modelling & Software*, Volume 13, 193 – 209, (1998).
115. Zhang, Z. and Friedrich, K., (2003). Artificial neural network applied to polymer composites: a review, *Composites Science and Technology*, 63(14), 2029-2044.
116. Jiang, Z., Zhang, Z. and Friedrich, K., (2007). *Composites Science and Technology*, Volume 67, Issue 2, 168-176,
117. Veeresh Kumar, G. B., Rao, C. S. P., Selvaraj, N., (2011). *Journal of Minerals & Materials Characterization & Engineering*, Vol. 10, No.1, 59-91
118. Rashed, F.S., Mahmoud, T.S., *Tribology International* 42 (2009) 642–648.
119. William, F. H, (2005). *Mechanical behavior of Mat.*, Cambridge Uni. Press, UK.
120. Ruff, A.W and Ives, L.K, (1975). Measurement of solid particle velocity in erosive wear. *Wear*, 35(1), 195–9.
121. Modi, O.P. Prasad, B.K., Influence of alumina disperoid and test parameters on erosive wear behavior of a cast zinc-aluminium alloy. *WEAR*, 260, 895-902
122. Zeng, P, (1998). Neural Computing in Mechanics, *Appl. Mech.*, 51 (2), 173–197.
123. Kadi, H. E, (2006). Modeling the Mechanical Behavior of Fiber-Reinforced Polymeric Composite Materials using Artificial Neural Networks—A Review, *Composite Structures*, 73 (1), 1-23.
124. Haykin, S, (1999). *Neural Networks: a Comprehensive Foundation*, Upper Saddle River, Prentice Hall, NJ, USA.
125. Rumelhart, D.E., Hinton, G., Williams, R., (1986). in: D.E. Rumelhart et al. (Ed.), *Parallel Distributed Processing*, vol. 1, MIT Press, Cambridge, MA, USA, , 318.
126. Genel, K., Kurnaz, S. C., Durman, M., (2003). Modeling of tribological properties of alumina fiber reinforced zinc–aluminum composites using artificial neural network, *Materials Science and Engineering A363*, 203–210.

APPENDICES

Appendix - A1**List of Publications out of this Work****International Journals**

1. **Srimant Kumar Mishra**, Sandhyarani Biswas, Alok Satapathy and Amar Patnaik, *Erosion Wear Analysis of Al_2O_3 Particles Reinforced ZA-27 Alloy Metal Matrix Composite Using ANN*, Accepted for publication in **International Journal of Materials, Manufacturing and Design**.
2. **Srimant KU Mishra**, Sandhyarani Biswas, Alok Satapathy and Amar Patnaik, *Study of Erosion Wear Characteristics of ZA-27 Alloy Metal Matrix Composite Reinforced with SiC Particles Using ANN*, Communicated to **Proceedings of the Institution of Mechanical Engineers, Part J, Journal of Engineering Tribology**.

List of Papers Presented/communicated in Seminars/Conferences

1. **Srimant Kumar Mishra**, Sandhyarani Biswas, Alok Satapathy and Amar Patnaik, *Solid Particle Erosion Response Simulation of Alumina Reinforced ZA-27 Metal Matrix Composites*, Proceedings of the **International Conference on Mechanical Engineering 2011 (ICME2011)**, 18-20 December 2011, BUET, Dhaka, Bangladesh.
2. **Srimant Kumar Mishra**, Sandhyarani Biswas and Alok Satapathy, *Parametric Optimization of Erosion Wear Process of SiC Reinforced ZA-27 Metal Matrix Composites Using Taguchi Experimental Design*, Proceedings of the **IEEE – International Conference on Advances in Engineering, Science and Management (ICAESM-2012)**, March 30-31, 2012, Nagapattinam, Tamilnadu, India.
3. **Srimant Kumar Mishra**, Sandhyarani Biswas and Alok Satapathy, *Parametric Optimization in Solid Particle Erosion of Alumina Reinforced ZA-27 Metal Matrix Composites using Taguchi Experimental Design*, Communicated to the **Fifth International Conference on Solidification Science and Processing (ICSSP5-2012)**, November 19-22, 2012, Bhubaneswar, INDIA.
4. **Srimant Kumar Mishra**, Sandhyarani Biswas, Alok Satapathy and Amar Patnaik, *Wear Response Simulation of ZA-27 Metal Matrix Composites Using Artificial Neural Network*, Proceedings of the **National Conference cum Workshop on Recent Developments in Engineering Materials (RDEM-2011)**, May 2011, Birla Institute of Technology, Mesra, Ranchi, India.
5. **Srimant Kumar Mishra**, Sandhyarani Biswas and Alok Satapathy, *A Study on Erosion Wear of SiC Reinforced ZA-27 Metal Matrix Composites Using Taguchi Experimental Design*, Proceedings of the **National Conference on Processing and Characterization of Materials (NCPCM-2011)**, 2-3 December, 2011, National Institute of Technology, Rourkela, India.

Appendix – A2**Brief bio-data of the author**

The author, **Srimant Kumar Mishra**, born on 17-07-1986 graduated in Mechanical Engineering from Biju Patnaik University of Technology (BPUT) in the year 2008. Before joining the M.Tech. (Research) programme at the National Institute of Technology, Rourkela, he had served as a faculty in the Department of Mechanical Engineering at Black Diamond College of Engineering and Technology, Jharsuguda and then as a Research Project Assistant at CSIR Lab, Bhubaneswar.

During his tenure at the CSIR Lab., he was working in the field of plasma spray coating and material characterization. He has authored 02 research papers in international journals and has also presented 04 research papers at various national and international conferences. In the postgraduate programme, he has worked in the area of erosion wear behaviour of particulate filled metal matrix composites.
